University of South-Eastern Norway

www.usn.no

FM4017 PROJECT

# ONLINE VOLTAGE STABILITY MONITORING BY PMU FOR AC GRIDS WITH HVDC-CONNECTED OFFSHORE WIND GENERATORS

GROUP MP-18-21

Faculty of Technology, Natural Sciences and Maritime Sciences
Campus Porsgrunn

University of South-Eastern Norway

www.usn.no

**Course**: FM4017 Project

**Title**: Online voltage stability monitoring by PMU for AC grids with HVDC-connected offshore wind generators

**Number of pages:** 63

**Keywords:** Offshore Windfarm, VSC-HVDC, PMU, Voltage Stability, Quasi steady state stability, Pulse width modulation (PWM), Load and Thevenin impedance matching.

**Project:** Group MP-18-21

**Group participants:** Dhanush Wagle - 238810
Muhammad Akhlaq - 238811
Okwo Oluchi Mercy - 238802

**Supervisor:** Jalal Khodaparast

**Summary:**

Offshore wind power, an alternative source of electrical energy has been of a major concern over the years due to its availability and strength compared to that of the onshore wind power. Its demand has increased the use of HVDC technology in the ac/dc integration. However due to the disturbances experience with wind power generation, there is need for the online monitoring of voltage stability in the power system.

In response to that, a HVDC model is proposed for a voltage instability as a case study. The Phasor measurement unit is connected at both stations of the VSC to measures the HVDC parameters. Introducing the HVDC modelled circuit to an online voltage instability detection by Thevenin impedance matching, the voltage instability margin can be evaluated.

This process is being validated using DIgSILENT PowerFactory to simulate an offshore windfarm connected to a VSC-HVDC converter and with a 9 Bus System as a grid.

# Preface

This report contributes the final work for course FM4017-1 21H Project of Master of Science Electric Power Engineering, at the Department of Electrical Engineering, It and Cybernetic at the University of South-Eastern Norway (USN).

The purpose of this project is to study the voltage instability using PMU when the VSC-HVDC connected offshore windfarm is integrated to the grid.

We would like to thank our supervisor, Associate Professor Jalal Khodaparast, for the supervision, expert guidance, and helpful insights during the work with the project.

November 19, 2021, Porsgrunn

Dhanush Wagle
Muhammad Akhlaq
Okwo Oluchi Mercy

# Contents


**Preface** ..... 3

**List of Figures** ..... 6

**List of Tables** ..... 8

**1 Introduction** ..... 9

1.1 Background ..... 9
1.2 Objectives ..... 10
1.3 Method ..... 10
1.4 Scope ..... 10
1.5 Report Structure ..... 10

**2 Theory** ..... 11

2.1 Wind Energy ..... 11
2.2 Calculation of Wind Power: ..... 11
2.3 Wind Turbine ..... 12
*2.3.1 Type A: Fixed Speed Wind Turbine* ..... *13*
*2.3.2 Type B: Limited variable speed:* ..... *15*
*2.3.3 Type C: Variable speed with partial scale frequency converter:* ..... *15*
*2.3.4 Type D: Variable speed with full scale frequency converter:* ..... *16*
2.4 The dynamics of a DFIG: ..... 16
2.5 Wind farm layouts ..... 18
*2.5.2 General wind farm layout* ..... *18*
*2.5.3 AC layouts for wind farms* ..... *19*
*2.5.3 AC/DC mixed layouts for wind farms* ..... *19*
2.6 Offshore Wind Farm Connection System ..... 20
*2.6.3 Offshore collection system* ..... *20*
*2.6.4 Transmission Link to the Shore* ..... *20*
2.7 Phasor Measurement Unit (PMU) ..... 20
*2.7.3 Synchro phasor* ..... *21*
*2.7.4 Basic PMU structure* ..... *21*
2.8 Phasor Estimation Technique ..... 23
*2.8.1 Zero Crossing* ..... *24*
*2.8.2 DFT:* ..... *24*
*2.8.3 Sliding DFT* ..... *25*
2.9 TRANSMISSION SYSTEM FOR OFFSHORE WIND FARM ..... 25
*2.9.1 HVAC TECHNOLOGY* ..... *26*
*2.9.2 HVDC TECHNOLOGY* ..... *27*
2.10 HVDC TOPOLOGY ..... 31
*2.10.1 LCC-HVDC* ..... *31*
*2.10.2 VSC-HVDC Converter* ..... *33*
2.11 Quasi Steady State ..... 36
*2.11.1 Definition and Basic Principle* ..... *36*
*2.11.2 QSS Model of VSC-HVDC Link* ..... *37*
2.12 Voltage Instability Detection ..... 39
*2.12.1 Power System Stability* ..... *39*
*2.12.2 Thevenin Equivalent of an HVDC-Connected Offshore Wind Farm* ..... *41*
*2.12.3 Voltage Instability Detection* ..... *43*

**3 Network Definition in DIgSILENT Power Factory** ..... 44

3.1 VSC-HVDC Transmission System ..... 44
3.2 DFIG Wind Farm ..... 45

3.3 9 Bus System ..... 47
4 Simulations and results ..... 49
5 Summary ..... 53
5.1 Conclusion ..... 53
5.2 Future Work ..... 53
Reference ..... 55
Appendices ..... 58

# List of Figures

Figure 1-1: VSC-HVDC connected offshore wind farm ..... 9
Figure 2-1: Mechanical components of wind turbine ..... 13
Figure 2-2: Electrical components of wind turbine[2] ..... 13
Figure 2-3: Type A configuration: Fixed speed control[3] ..... 14
Figure 2-4: Type B configuration: Limited variable speed control ..... 15
Figure 2-5: Type C configuration: Variable speed control with partial scale converter ..... 15
Figure 2-6: Type D topology: Variable speed control with full scale frequency converter ..... 16
Figure 2-7: Electrical scheme of DFIG[3] ..... 16
Figure 2-8:AC/DC Mixed Layout ..... 20
Figure 2-9: Basic PMU Structure ..... 22
Figure 2-10: Sinusoidal signal with its phasor ..... 23
Figure 2-11: HVAC transmission system [14]. ..... 26
Figure 2-12: Comparison for HVDC and HVAC capital cost[15] ..... 27
Figure 2-13: Schematic diagram of a HVDC system [16]. ..... 28
Figure 2-14: Back-to-back CSC-HVDC system with 12-pulse converters [16] ..... 28
Figure 2-15: Monopolar CSC-HVDC system with 12 pulse converters [16]. ..... 29
Figure 2-16: Bipolar CSC-HVDC system with one 12-pulse converter per pole [16] ..... 29
Figure 2-17: Multiterminal CSC-HVDC system—parallel connected [16]. ..... 29
Figure 2-18: Single line diagram of a monopolar HVDC converter station [17]. ..... 30
Figure 2-19: (a) Three phase two winding (b) single phase two winding (c) single phase three winding (d) three phase three winding [18] ..... 30
Figure 2-20: The 12-pulse LCC–HVDC system [19]. ..... 31
Figure 2-21: Thyristor ..... 32
Figure 2-22: Graetz circuit ..... 32
Figure 2-23: Simplified circuit diagram of a VSC HVDC [23]. ..... 33
Figure 2-24: Pie model of a single pole for a dc-transmission link ..... 34
Figure 2-25: (a) VI Characteristics (b) Symbol ..... 34
Figure 2-26: PWM switching signal ..... 35
Figure 2-27: Basic circuit for PWM ..... 35
Figure 2-28: Output Waveform of PWM ..... 35
Figure 2-29: QSS model of point-to-point VSC-HVDC link [29] ..... 38

Figure 2-30: Classification of Power System Stability [25] ..... 39
Figure 2-31: Thevenin equivalent circuit [31] ..... 41
Figure 2-32: Phase difference between load and Thevenin impedance ..... 42
Figure 2-33: Equivalent circuit of an HVDC-connected offshore wind farm [29] ..... 42
Figure 3-1: PowerFactory model of VSC-HVDC line ..... 44
Figure 3-2: PowerFactory Model of DFIG Wind Farm ..... 45
Figure 3-3: Detailed Feeder for 10 DFIGs ..... 46
Figure 3-4: Single Busbar with Tie ..... 47
Figure 3-5: Single line diagram of the Nine-bus System ..... 47
Figure 4-1: Load flow calculations on 9 bus system ..... 50
Figure 4-2: Voltage Profile ..... 50
Figure 4-3: Voltage profile after events ..... 51
Figure 4-4: Thevenin vs load Impedance ..... 52

# List of Tables

Table 1: AC Wind turbine Concept ..... 13
Table 2: Parameters of the 3-winding transformer ..... 58
Table 3: Parameter of the VSC-Converter ..... 58
Table 4: Parameter of the HVDC Line ..... 59
Table 5: Parameter of three phase transformer ..... 59
Table 6: Parameters of 5-MW DFIG ..... 59
Table 7: Parameters of Three Phase Transformer ..... 60
Table 8: Parameters of NEC ..... 60
Table 9: Nominal Bus Voltages ..... 61
Table 10: Generator Data ..... 61
Table 11: Load Data ..... 62
Table 12: Line Data ..... 62
Table 13: Transformer Data ..... 63
Table 14: Event list of cascading failures ..... 51

# 1 Introduction

## 1.1 Background

Over the years, there has been an overdependent on the use of fossil fuels as the major source of energy in the world. With the rise in oil price and environmental pollution of $CO_2$ and other greenhouse gases released into the environment because of increase in population and production respectively, thus there is need for alternative source of energy.

Offshore wind farms, one of the renewable energy sources, have grown in popularity because greenhouse gas emissions should be minimized and the increase in power generation from renewable energy sources such as wind. This established goal has expanded not just the quantity of offshore wind farms, but also the utilization of VSC-HVDC for ac/dc integration. Because of the greater availability and strength of offshore wind compared to onshore wind, the focus of wind energy development has shifted to offshore wind farms.

However, because of the power loses over a long-distance during transmission of wind energy from the offshore to the mainland, Voltage source converter- High voltage direct current (VSC-HVDC) technology is used to integrate the offshore wind farm to the ac grid compared to the High voltage alternating current (HVAC) system of transmission. There is need for online voltage monitoring of offshore wind power due to the fluctuations in wind and generator dynamics experienced during wind energy production.

Voltage stability is the ability of a power system to maintain a certain level of voltage balance at all buses during steady state operation and after being subjected to a disturbance. Voltage Stability Assessment (VSA) using the phasor measurement unit (PMU) has gain popularity in the past few years due to its ability to measure in real time, using the measured values to estimate the Thevenin's equivalent impedance and comparing with the load impedance for stability assessment. In this project, a VSC-HVDC model is designed using the PMU technology to monitor online the voltage instability of an AC grid connected to a HVDC-connected offshore wind generator as shown in figure 1-1.

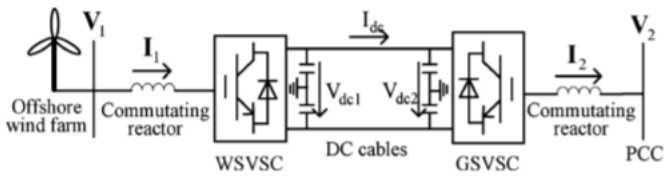


Figure 1-1: VSC-HVDC connected offshore wind farm

## 1.2 Objectives

The main objective of this project is to model a VSC-HVDC and wind farm for a voltage stability analysis based on circuit theory and simulate the system in DIgSILENT PowerFactory.

Phasor measurement unit (PMU) is used to measure power system phasor quantities in real time for an online voltage instability analysis based on Thevenin's impedance matching.

## 1.3 Method

Quasi-steady state approximation is used for the long-term dynamic analysis of the whole power system for the calculation of Thevenin and Load impedances.

DIgSILENT PowerFactory is used for design of the whole system, then the RMS Simulation is carried out to find the voltages and currents which then was transferred to MATLAB for further signal processing to find the difference in the magnitude of Thevenin and Load impedances for voltage stability analysis.

## 1.4 Scope

a) Study area: The project is carried out in HVDC-Connected Offshore Wind Farm and 9 Bus System.
b) Tools: PowerFactory is utilized to model and run the simulations, while Microsoft Excel and MATLAB are used to analyse and plot graphs from the.csv files acquired by PowerFactory.
c) Timeline: From 27th August 2021 to 19 November 2021.
d) Supervision: Associate Prof. Jalal Khodaparast, the supervision conducted meeting twice a month for supervision and guidance.
e) Documents: The supervisor has provided the necessary papers, books as helping materials.

## 1.5 Report Structure

Chapter one discusses the background of the project.

Chapter two discusses the theories and the different methodologies.

Chapter three defines the grid networks used for simulation.

Chapter four describes the simulations and explains the results.

Chapter five attempts to conclude the work in this project.

# 2 Theory

## 2.1 Wind Energy

In recent years throughout the world wind energy is obtaining attention day by day. Renewable energy resources like wind energy are native and help to reduce dependences on other fossil fuels. Wind is generated by the sun as the light of sun is not same across the whole world. Some areas of the world are colder, and some are warm. So, temperature differential of the earth surface helps to create wind. According to the rough estimate 10-million-watt energy can be produced by the wind on this earth. Wind energy is resource efficient option when the other natural fossil fuels of the world are decreasing day by day. Wind energy is defined as the conversion of wind Kinetic energy into electric energy by a wind turbine.[1]. The power curve is used to explain the wind power which is sometimes dependent on site setting and turbine model. s. Most wind turbines begin producing electricity at roughly 4 m/s (9 mph), achieve rated power at around 13 m/s (29 mph), and then stop producing power at around 25 m/s (56 mph)[2]. Wind energy depends on three factors:

1)**Wind Speed:** The power produce by the wind is the cube of wind speed. Its means that the power will be 8 times if the wind speed is twice($2^3$=2x2x2=8). In other words the site where average breeze speed is 8m/s, the turbine will produce 75-100% more energy as compare to the site where speed is 6m/s.

2)**Wind turbine Availability:** this is the potential of the machine to work when the breeze is blowing. Normally in Europe this is 98 % or above.

3)**The way wind turbines are arranged:** Wind farms are designed in such a way that one wind does not affect the other turbines. Although grid connection, visibility and environmental consideration are also important parameter while designing wind farms.

## 2.2 Calculation of Wind Power:

The electrical design engineer should know the concept and understanding of complex and mathematical equations behind the designing of wind turbine generator. Along the concept of wind energy, they should also keep the following information in mind.

1)Output power is directly proportional to the area cover by the rotor. Its mean that if area is double then power will also be double.

2) The generator's output power is proportional to the wind speed cubed.[2]

$$K.E = \frac{1}{2} * m * v^2 \quad (1)$$

- Mass is measured in Kg
- Velocity is measured in m/s

- Energy is measured in joules

The air density at the sea level is 1.23kg/m$^3$. The following equation is used to find the mass of air hitting turbine per second.

$$\frac{mass}{sec} = Velocity * Area * Density \quad (2)$$

- Velocity in m/s
- Density in kg/m$^3$
- Area in m$^2$

For certain area in the wind the power (i.e., energy per second) is find by inserting the mass equation into kinetic energy equation. So, power equation is.

$$P = 0.5 * Area * Air\ Density * velocity^3 \quad (3)$$

- Area in square meter
- Air density in Kilogram per cubic meter
- Velocity in meter per second

The wind power equation is given by [2]

$$P = 0.5 * \rho * A * C_p * V^3 * N_g * N_b \quad (4)$$

- $\rho = Air\ Density\ \left[\frac{kg}{m^3}\right]$
- $A = Rotor\ swept\ Area[m^2]$
- $C_p = Coefficient\ of\ performance$
- $N_g = generator\ efficiency$
- $N_b = gear\ box\ bearing\ efficiency$

## 2.3 Wind Turbine

The speed of the wind turbine in not same either it is fix or variable. There are many approaches to control the power in wind turbines. In this section various approaches for speed and power control will explains and at the end standard AC types of wind turbine also explain. Moreover,

wind turbine also classified on the base of power control. Table 1 describe the different types of AC turbine wind configuration [3].

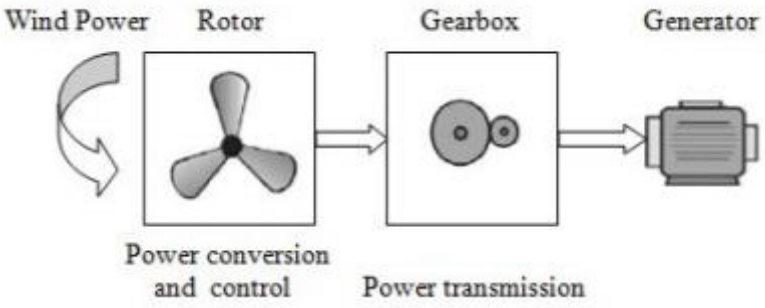


Figure 2-1: Mechanical components of wind turbine

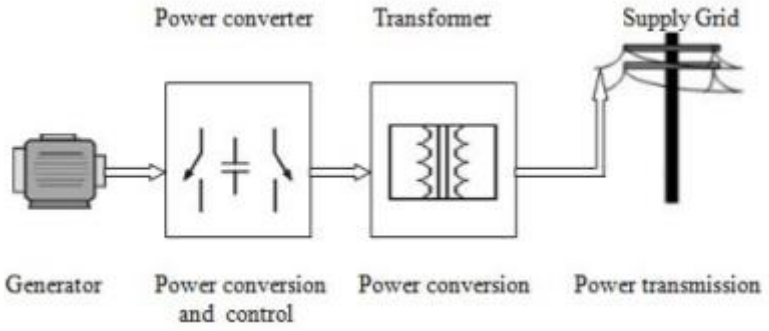


Figure 2-2: Electrical components of wind turbine[2]

Table 1: AC Wind turbine Concept

| Speed Control | | Power Control | | |
|---|---|---|---|---|
| | | Stall | Pitch | Active Stall |
| Fixed Speed | Type A | Type A0 | Type A1 | Type A2 |
| Variable Speed | Type B | Type B0 | Type B1 | Type B2 |
| | Type C | Type C0 | Type C1 | Type C2 |
| | Type D | Type D0 | Type D1 | Type D2 |

### 2.3.1 Type A: Fixed Speed Wind Turbine

The frequency of the supply grid gear ratio and the generator design determine the wind turbine's speed. Induction generators are commonly used to generate wind speed. It has a soft

starting for a more seamless connection to the grid.The Soft starter is a simple circuit used to reduce the inrush current and in this way the grid disturbance is limited. As usually the grid is connected to the generator and the reactive power drawn by the induction generator is compensated by a capacitor bank.

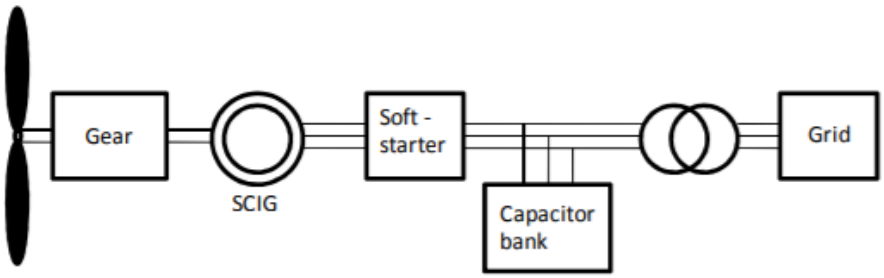


Figure 2-3: Type A configuration: Fixed speed control[3]

Type A wind turbine is used to control the power output. There are three concepts i.e. Stall control, Pitch Control and Active stall control.

**Type A0: Stall Control:**

In stall control the blades of the turbine are placed at a fixed angle. Install control the rotor is designed to generate the power when the wind is crossed the limit. On a positive side the design is simple, powerful, and affordable, whereas it has low efficiency on the low level of wind.

**Type A1: Pitch Control:**

The blades of the pitch control are moveable and can move into the wind as the output power is too high or too low. It has the advantage of improved control, aided start-up, and emergency stop. When the wind is strong, the mean output of this sort of generator remains near to the rated power of the generator. Due to high speed, there is large fluctuation.

**Type A2: Active Stall Control:**

The blade stall is controlled by the pitch of the blades in this type. In order to attain optimal efficiency at low wind speeds, the blades operate like a pitch-controlled wind turbine. Because of the smoother limited power, this kind does not encounter a large fluctuation with a high wind speed. It is easy to stop and start in case of emergency due to the combination with pitch control type.

#### 2.3.1.1 Variable Speed wind Turbine

In order to attain the greatest power coefficient, a variable speed wind turbine maintains a constant speed tip ratio. This is accomplished by adjusting the turbine's rotating speed as the wind changes. The variable-speed wind turbine is usually connected to a synchronous generator and then synchronized with the grid via a power converter.Better power quality, less mechanical stress on the turbine and more energy capture by the variable wind speed.

### 2.3.2 Type B: Limited variable speed:

A wound rotor induction generator with a variable rotor resistance makes up the limited variable speed generator. OptiSlip is the name for this rotor reluctance. It is controlled by an optically controlled converter mounted on the rotor shaft. The generator is synchronized with the grid by transformer, Capacitor bank and soft starter.

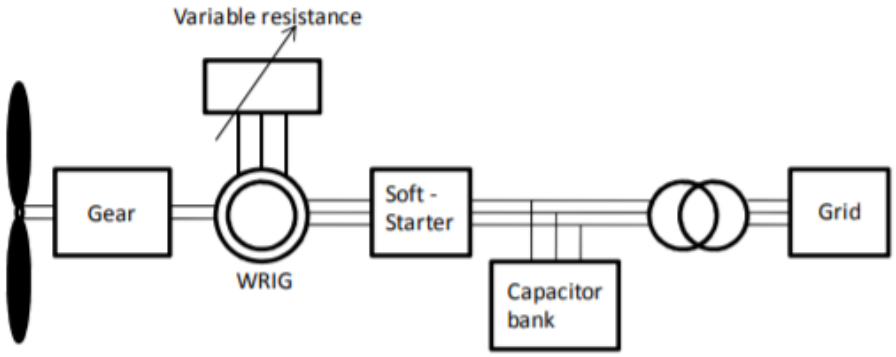


Figure 2-4: Type B configuration: Limited variable speed control [3]

By controlling the rotor resistance, the output power is also controlled. Overall, this topology is simple and easy to use.

### 2.3.3 Type C: Variable speed with partial scale frequency converter:

Doubly fed induction generator is the name for this topology (DFIG). The wound rotor induction generator (WRIG) is directly connected to the grid via a transformer in this type.The rotor circuit is fitted with a partial scale frequency converter, which ensures a trouble-free connection along the reactive power correction provided by the soft starter and capacitor bank.

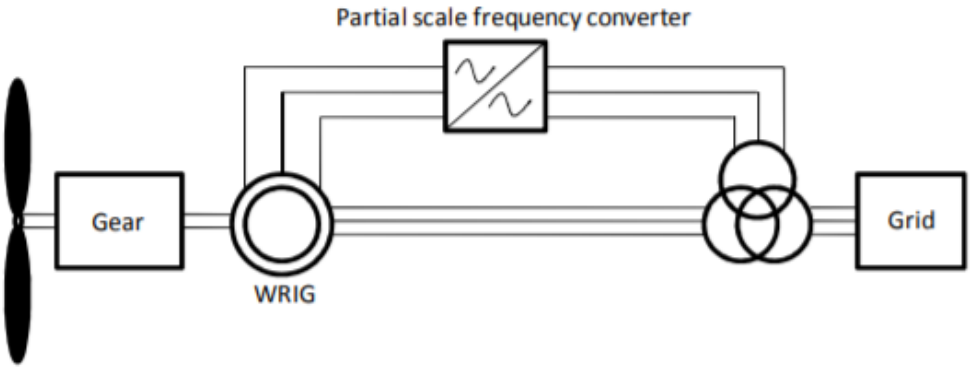


Figure 2-5: Type C configuration: Variable speed control with partial scale converter [3]

The DFIG eliminates the need for magnetizing the generator from the grid, as the active and reactive power is decoupled. The main advantages are the elimination of the need for brushes and maintenance, which is vulnerable to grid failures.

### 2.3.4 Type D: Variable speed with full scale frequency converter:

In this type of the permanent magnet is used to excite the generator. Converter ensures that the grid connection is smoother and compensates for reactive power.

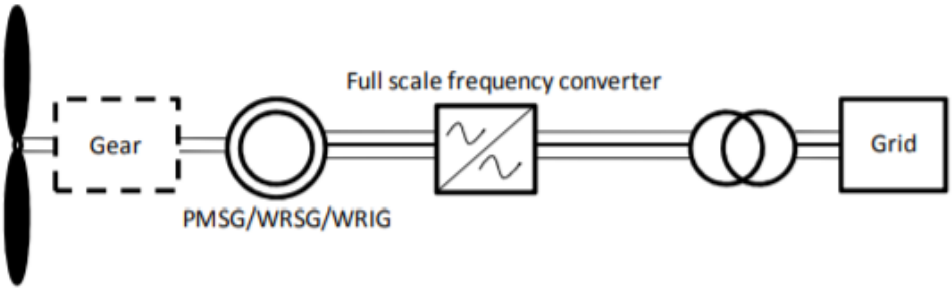


Figure 2-6: Type D topology: Variable speed control with full scale frequency converter [3]

## 2.4 The dynamics of a DFIG:

In this project DFIG model is used for simulation. DFIG can increase the angular behaviour of the wind system, but it also decreases the voltage margin under large disturbances. The DFIG with power system stabilizer is used as power system damping.

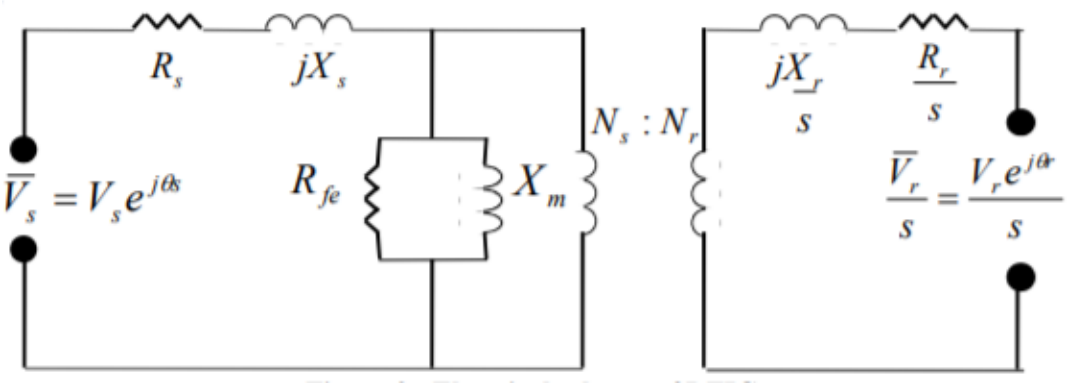


Figure 2-7: Electrical scheme of DFIG [3]

Stator side values are represented by values with s and rotor side values by values with r. [3]

- $V = Voltage[V]$

- $\theta_s = Voltage\ phase\ angle[°]$
- $\theta_s = Angular\ displacement\ between\ stator\ and\ rotor\ voltage[°]$
- $R = Resistance[\Omega]$
- $X = Reactance[H]$
- $N = no\ of\ windings$

S is the slip which is given by the following equation.

$$s = 1 - \frac{\omega_r}{\omega_s} \tag{5}$$

- $\omega_s = Rotational\ Speed\ of\ the\ stator\left[{}^{rad}/_{s}\right]$
- $\omega_r = Rotational\ speed\ of\ the\ rotor\left[{}^{rad}/_{s}\right]$

A DFIG's dynamics can be described by two axial models, with no compensation in the form of voltage regulation, using equations of the third order.

$$\delta' = \frac{1}{\mathrm{E'T_0}}(-\mathrm{T_0}(\omega_\mathrm{s} - \omega_\mathrm{r})\mathrm{E'} - \frac{\mathrm{X_s} - \mathrm{X'}}{\mathrm{X'}}\mathrm{V_s}\sin(\delta - \theta_\mathrm{s}) + \mathrm{T_s}\omega_\mathrm{s}\mathrm{V_r}\sin(\delta - \theta_\mathrm{r}) \tag{6}$$

$$\omega_r` = \frac{1}{M}\left(P_m\frac{\omega_s}{\omega_r} - P_e\right) \tag{7}$$

$$E`_q = \frac{1}{T_0}(T_0\omega_s V_{dr} - T_0(\omega_s - \omega_r)E`_d - \frac{X_s}{X`}E`_q + \frac{X_S - X`}{X`}V_q \tag{8}$$

$$E`_d = \frac{1}{T_0}(T_0\omega_s V_{dr} - T_0(\omega_s - \omega_r)E`_d - \frac{X_s}{X`}E`_q + \frac{X_S - X`}{X`}V_q \tag{9}$$

$$P_e = \frac{E`V}{X`}\sin(\delta - \theta_s) = v_{ds} - i_{ds} + v_{qs}i_{qs} = P_s \tag{10}$$

$$X` = X_s - \frac{X^2{}_m}{X_r} \tag{11}$$

$$T_0 = \frac{X_r}{\omega_s R_r} \tag{12}$$

$$M = \frac{2HS_n}{\omega_s} \tag{13}$$

- $\delta =$ Angle between transient emf and stator voltage [°]
- $E` = Transient\ Emf[V]$
- $T_0 = Open\ circuit\ time\ constant\ [s]$
- $\omega = rotational\ speed\ [rpm]$
- $X` = Transient\ reactance[H]$
- $M = inertia\ coefficient[MVAS^{-2}]$
- $P_m = mechanical\ output\ power\ [W]$
- $P_e = electrical\ output\ power[W]$
- $P_s = Stator\ power\ [W]$
- $H = inertia\ constant\ of\ turbine\ shaft\ and\ generator[s]$
- $S_n = Transient\ Reactance\ [MVA]$

## 2.5 Wind farm layouts

There are many options for the wind farm layout according to the transformer and power electronics utilization. Following are some layouts of wind farm.

### 2.5.2 General wind farm layout

The following are the elements of this wind farm:

- Wind turbines
- Local wind turbine grid
- Collecting point
- Transmission system

- Wind farms interface to the point of common coupling (PCC)

Wind turbine consists of generator, Power electronics and transformer and the collecting point is the offshore substation which is consists of transformer and power electronics components. The wind farm grid modifies all parameters according to the power demand at the PCC.

## 2.5.3 AC layouts for wind farms

The grid connection and transmission systems for the present wind farms are all built on AC technology. So, there are two approaches for AC layout for wind farms i.e., small, and large AC wind farm.

### 2.5.3.1 Small AC wind farm

In this topology, the wind farm transports both power from the source to the consumer as

well as connecting the turbines.

The production level of voltage is dependent on the distance between the shore and wind farm.

### 2.5.3.2 Large AC wind farm

An AC wind farm involves connecting the turbines to offshore substations and then transferring the power from the substations to the onshore grid. To minimize the transmission losses in offshore substation the voltage regulator and reactive power compensation devices are placed to adjust the different parameter before transfer to the local grid.

## 2.5.3 AC/DC mixed layouts for wind farms

Wind turbines connected to an offshore AC grid that is collected at an offshore station are used in mixed AC/DC systems. An HVDC solution is used to transfer the power to shore from this station. On shore, the power is converted back to AC and fed back into the grid.[3]

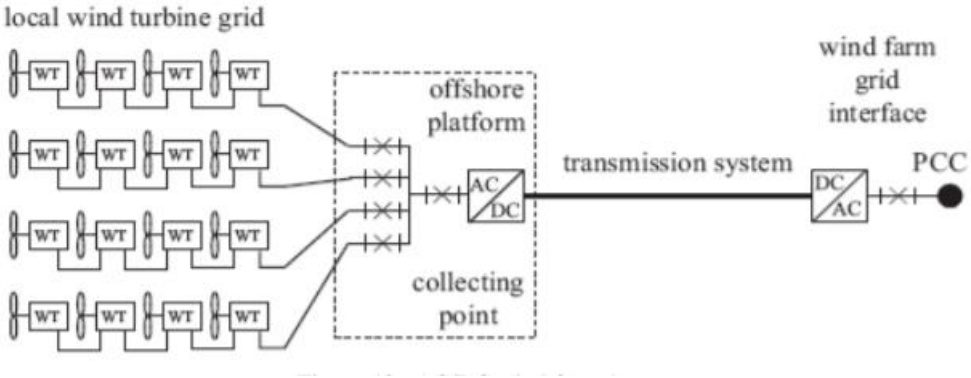


Figure 2-8:AC/DC Mixed Layout

If the distance between the onshore grid and offshore grid is long, then topology is best.

## 2.6 Offshore Wind Farm Connection System

Electrical connection of wind farm can be categorized into offshore collection and transmission system to the shore.

### 2.6.3 Offshore collection system

In the offshore system, the wind turbines generate all their power and feed that directly into the main grid. A star or string cluster topology is usually used for collection points. A string cluster is an arrangement of wind turbines that deliver power to the feeder, where a high level of voltage allows the power to flow into the strings. To follow the voltages of generators and feeders, step-up transformers are required at each wind generator. Whereas for star cluster all the turbine is directly attached with nodal point. In this point, the power is transferred to the central collection point, and the voltage level is further enhanced, so this is where the transformer is located. Moreover, in star cluster step up transformer does not require separately whereas it need multiple collection points for switchgear and transformer.

Currently string cluster is used across all over the world for offshore wind farms.

### 2.6.4 Transmission Link to the Shore

The transmission link to the shore from the offshore collection point can be HVAC, HVDC using thyristor-based line commutated converters (LCC), or VSC-HVDC. All existing wind farms were using the HVAC connection as a solution[4]

## 2.7 Phasor Measurement Unit (PMU)

A phasor measurement unit is a device that measures voltage and current at various points in a power system. PMU measure the data as phasor in complex form which are the magnitude and angle of the sine wave. To find the phase different parameter, the phasor estimation technique

is utilized. The measured data must be correct in order to implement this procedure. Therefore, PMU has a lot of importance in power system mechanism such as for the protection of system, state estimation and post fault analysis. The cost of PMU is very high so in power system optimally place where PMU will be installed and observe all power system is favourable research topic in across the world. The phase of various parameters is estimated using phasor estimating techniques such as zero crossing, DFT, and SDFT. PS is also used for time stamping to get the accurate information of the power system. Online application of PMU is monitoring the of stability voltage current and frequency as well as detection of any harmonics in the grid. Whereas offline application contains post fault analysis ,validating model and data compilation.[5]

### 2.7.3 Synchro phasor

A phasor is complex number having the signal attributes like the magnitude and phase. The word synchro phasor means that synchronization of the all-phasor measurement. The mathematical form of pure sinusoidal signal is given by the following equation.

$$X(t) = Xm\cos(wt + \emptyset) \quad (14)$$

- $Xm = \text{magnitude of the signal}$
- $\omega = 2\pi f \; is \; the \; frequency \; of \; the \; signal$
- $\emptyset = Angle \; of \; the \; signal$

Universal time coordinate as time reference is used in synchro phasor. Phasors mean the sinusoidal signal which is obtained by the phase difference of original signal and reference signal.so the two signal directly compare the same reference.

### 2.7.4 Basic PMU structure

PMU works as observing device in the power system. It observes the phase of current, voltage and frequency of a node. The block diagram of the PMU is given below.[6]

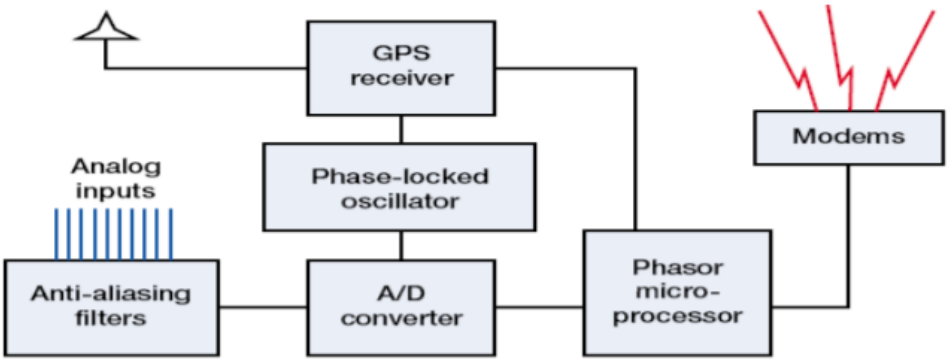


Figure 2-9: Basic PMU Structure

The PMU consists of three parts

- Clock Synchronization Unit
- Measurement Unit
- Data transmission unit

The clock synchronization unit contains of GPS receiver and phase locked oscillator which are used to give the sampling clock of the measurement. The GPS source send the 1 pulse per second synchronizing signal to the GPS receiver. Both the GPS source and phase locked oscillator give the synchronized sampling of 1 micro second accuracy.[6] [7].A PLL is a control system which generate the output signal and the phase of that signal is exactly same with the input signal. Variable frequency oscillator and phase detector are parts of the PLL. The phase detector helps in comparing the phase of input signal and output signal whereas the oscillator is used to generate the periodic signal. The measurement unit has been further subdivided into three parts.

- Anti -Aliasing Filter
- Analogue to Digital Converter
- Phasor measurement unit/Processor

An anti-aliasing filter apply on the signal before sampling and for checking the sampling algorithm and limit the bandwidth of the signal. The interpretation of the signal is possible only if the signal satisfies the Nyquist rule. A low pass filter is often used to combat aliasing, but it is not necessary. For signals which are not cantered at zero but bandwidth signals and for that signal. For signals which are not cantered at zero but bandwidth signals and for that signal an anti-aliasing filter is used in conjunction with a band pass filter. After the filter the signal is directly fed into the ADC.ADC is a device in which the continuous

physical quantity such as time and amplitude are converted into discrete time and discrete amplitude with the help of sampling converter. PMU are installed on a large scale to observe the whole power system by the use of measured data. To gain such large installation PMU are integrated with microprocessor which is consists of relays. For the phasor estimation various tools are used like MATLAB, and LabView.

Measurement unit data is transmitted to the communication module via the communicatio ns protocol, such as modem, by the data transmission unit.

## 2.8 Phasor Estimation Technique

Phasor is used to the represent the sinusoidal AC voltage signal and it has the voltage and phase angle of the signal. The phasor will help to describe the behaviour of the power system even in instability region. So, the phasor of the signal helps the operator to reach the stability of grid. For example When the voltage and current of the power system along the frequency are not In the stability region or nominal value due to some harmonics then phasor will help to describe the performance of the power system.[8],[9].A sinusoidal signal represent the phase and voltage .

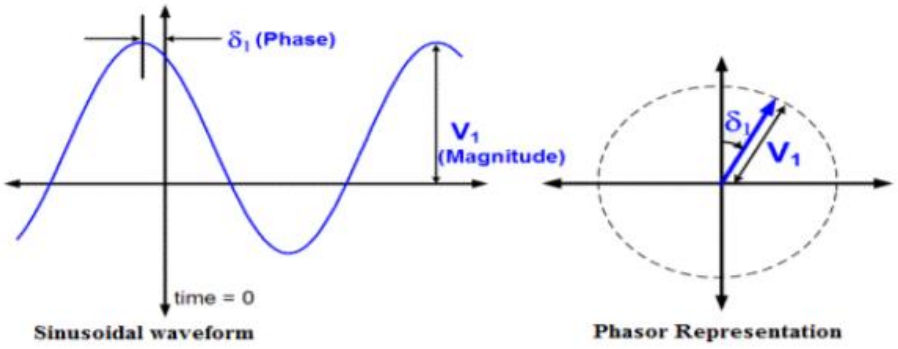


Figure 2-10: Sinusoidal signal with its phasor [5]

The phasor duration is proportional to the signal's RMS value, although the phase angle is arbitrary.

Here $\vartheta$ is used to represent the phase angle and define as angular measure like radian degree. So, the $\vartheta$ is negative if it's on the left side of the maximum value and vice versa.

Here below is some method which are used to estimate the phasor.

- Zero Crossing
- Discrete Fourier Transform (DFT)
- Sliding discrete Fourier Transform (SDFT)
- Least error square

- Kalman Filter
- Demodulation
- Phasor measurement angle changing

Zero crossing, DFT, and SDFT are mostly used for phasor estimation. So, in this project only focus on these.

### 2.8.1 Zero Crossing

Phase difference algorithm is implemented with zero crossing to find the phase. In this algorithm the time instant is observed when the measured and reference signal is crossed the zero. This instant helps to estimate the phase. Before the detection of zero crossing level in order to prevent the additive zero crossing due to additive noise and signal harmonic component the signal preconditioning is required.

In this method sinusoidal signal and measured signal are multiplied with each other. The frequency of the signal should be same. Mean or component value is obtained by the multiplication.$\tan^{-1}\left(Im\frac{X_n}{ReX_n}\right)$ function helps to find the phase difference of the two signal. The phase difference between the second signal and the reference signal can also be determin ed using the same method. So, the phase difference of the two buses is

$$\varphi = \varphi_2 - \varphi_1 \tag{15}$$

Two synchronized 50 Hz signals are created at two distinct buses to measure the phase angle between them, and the phase angle is then calculated by detecting the zero crossing of the reference signal and voltage signal.[10]

### 2.8.2 DFT:

DFT technique is also popular for phase estimation. There are two algorithms used in DFT i.e., Recursive Algorithm and non. Recursive algorithm.

In non-recursive algorithm data from previous window does not used and only fresh data take into account for finding the phase.[11]

A sinusoidal input signal with frequency $\omega$ [10].

[12]$x(t) = \sqrt{2}\text{Sin}\,(\omega t + \varphi)$

X is used to represent the phasor

$$X = Xe^{j\theta} \tag{16}$$

To convert the signal into discrete the signal is sampled is N times per cycle.

$$x_n = \sqrt{2}\sin\left(\frac{2\pi n}{N} + \varphi\right) \tag{17}$$

The fundamental component of the discrete Fourier transform is[12]

$$X^n = \frac{\sqrt{2}}{N}\sum_{n=0}^{N-1} x_n \cos\left(\frac{2\pi n}{N}\right) + j\,\frac{\sqrt{2}}{N}\sum_{n=0}^{N-1} x_n \sin\left(\frac{2\pi n}{N}\right) \tag{18}$$

An algorithm in which the data of previous window is consider for phase is called recursive algorithm.

The input signal has a fundamental frequency component which is given as:

$$X^{n+1} = X^n + \frac{\sqrt{2}}{N(x_{N+n} - x_n)e^{-jn\theta}} \tag{19}$$

Digital Frequency Translation transforms signals from the time domain to the frequency domain. In both domains, the information remains unchanged. If one domain is known, then other one can easily find. The DFT of any signal can be find by the following equation

$$X(k) = \frac{1}{N}\sum_{n=0}^{N-1} x(n)e^{-\frac{j2\pi nk}{N}} \tag{20}$$

### 2.8.3 Sliding DFT

For real time spectral analysis, sliding DFT requires fewer computations than DFT, because t hey do an N-point DFT on time samples within the sliding window, while SDFT does N samples over a time scale within the sliding window. The technique used for the SDFT also called as DFT shifting theorem.it mean that if the time domain signal is x(n)the DFT windowed time domain sequence is x(k)then the DFT of that sequence is shifted by one sample is $x(k)e^{\frac{j2\pi k}{N}}.The$ original spectral component is mulitiplied by the $e^{\frac{j2\pi k}{N}}$ for time shifted.[12]

$$S_k(n) = S_k(n-1)e^{\frac{j2\pi k}{N}} - x(n-N) + x(n) \tag{21}$$

## 2.9 TRANSMISSION SYSTEM FOR OFFSHORE WIND FARM

Transmission of power has become increasingly important and demanding due to the increase demand of reliable energy sources. To transmit power over a long distance from the point of generation to a grid or between two national grids, can be achieved using the High Voltage Alternating Current (HVAC) transmission or High Voltage Direct Current (HVDC) transmission. However, each type has its own advantages and disadvantages as will be discussed in the subsequent sections

## 2.9.1 HVAC TECHNOLOGY

Many offshore wind farms transmit their power from offshore to the mainland using HVAC. A high voltage alternating current (HVAC)transmission system is a passive system which means that the power is transmitted directly from the generation station to the mainland by a step-up transformer which increases the voltage to minimize power losses, and by a step-down transformer at the distribution end [13].

The diagram below is an HVAC transmission system made up of:

i. The HVAC cables
ii. The transformers at both ends and
iii. The compensation unit

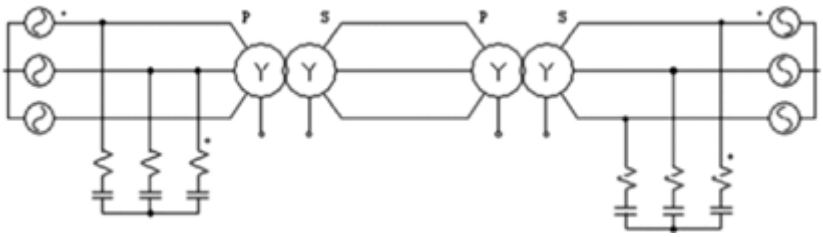


Figure 2-11: HVAC transmission system [14].

However, the HVAC transmission is faced with so many challenges which have contributed to its non-popularity in long-distance transmission of the offshore wind farm. The following are some of the setbacks [14]:

1. **Cost of transmission**: HVDC capital cost is higher than that of HVAC transmission for short distances below 600km (break-even point) but lower than the cost of HVAC transmission at a distance higher than 600km as shown in the figure below. This is because, at a short distance, the capital cost is higher in HVDC due to the introduction of the converters and inverter stations compared to that of HVAC whereas in distance longer the 600km, the cost of cable for an HVAC transmission is high compared to that of HVDC.

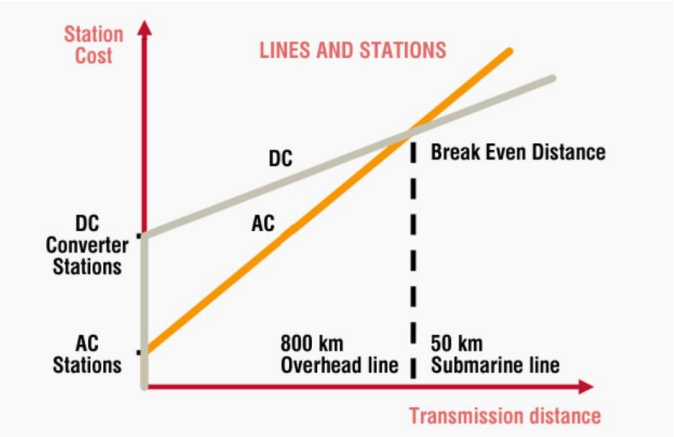


Figure 2-12: Comparison for HVDC and HVAC capital cost [15]

1. **Losses:** DC cable losses are lower than that of AC due to skin effect and corona effect which are less in DC cables, because of no changes in current with time as experienced in alternating current (AC). These two effects contribute to the increase in resistance of the AC than the direct current cable thus reducing the surface area for conductivity.

2. **Short circuit current:** when a fault occurs in the HVDC transmission line, the fault current is restricted from moving to the other parts of the power system which is contrary to that of the HVAC fault current. As a result, the fault current seems to be higher in HVAC than its HVDC counterpart.

3. **Interference with nearby communication lines:** HVAC has a frequency that interferes with nearby communication lines than that of HVDC.

4. **Asynchronous Interconnections**: HVAC does not support the interconnection of grids with different frequencies unlike that of HVDC where the Interconnection of Power grids of same or different frequencies is possible.

5. **Distance:** HVAC is affected by distance because of the power losses on a long transmission line compared to when a HVDC is used**.**

   From the discussion above, one can deduce that the main reason that affects HVAC transmission with respect to long-distance transmission is that a large amount of reactive power is lost and needs compensation on the reactive power from Flexible AC transmission systems (FACTS) such as SATCOM and SVC for its utmost performance. Thus, HVDC would be preferred in the integration of offshore wind farms to an Ac grid.

### 2.9.2 HVDC TECHNOLOGY

High voltage direct current is a device that transforms AC to DC as a rectifier and then transmits the DC after which the DC is then transformed from DC to AC as an inverter. HVDC technology was gradually introduced into the power sector from 1901-1999 by Hewitt's, who

first discovered the mercury-vapor rectifier for the transmission of DC power over a long distance followed by subsequent development on power electronics semiconductors to the development of Line commutated converter(LCC) - thyristor based also known as commutated current source converter(CSS) and Voltage Source Converter(VSC) – transistor based [16].

#### 2.9.2.1 System Overview (HVDC)

The diagram in figure 2-13 below is a schematic diagram of an HVDC system.

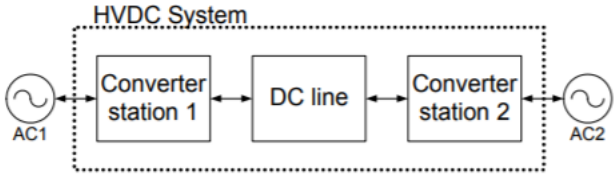


Figure 2-13: Schematic diagram of a HVDC system [16].

The HVDC system is made up of three main component parts namely:

i. **Converter station 1**: The converter station 1 acts like a rectifier, converting the Alternating current (AC) current from the Doubly fed induction generator (DFIG's) to a Direct Current (DC) which is transmitted to the DC - link.

ii. **Dc-Line:** converted DC current is transmitted through the line to the converter station two. It serves as an intermediary between the two converter stations.

iii. **Converter station 2:** This does the work of an inverter, transforming back the Direct current from the Dc-line to Alternating current (AC) at the distribution stations.

iv. **HVDC Configuration**

v. Depending on the function and operational use of the HVDC, they are configured in different ways. A typical example of a CSC – thyristor based HVDC is shown in the diagram below, same applies to a VSC – HVDC [16].

vi. Back-to-Back configuration: In back-to back- configuration, the rectifier and the inverter are in the same place likewise the 12 valves thereby reducing the length of the DC-link.

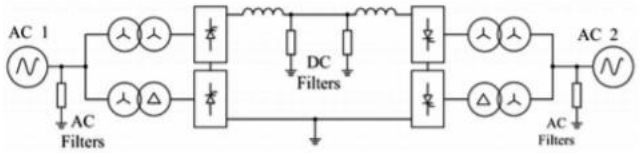


Figure 2-14: Back-to-back CSC-HVDC system with 12-pulse converters [16].

vii. Monopolar configuration: this arrangement makes use of the converters with one dc-line which could either be positive or negative dc voltage in-between and the earth as its current return path. They are mostly used in submarine connection.

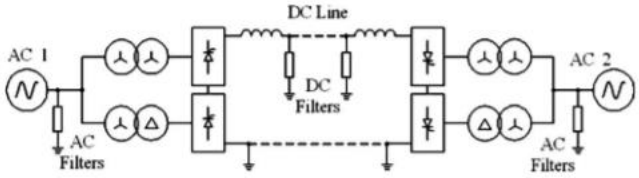


Figure 2-15: Monopolar CSC-HVDC system with 12 pulse converters [16].

viii. Bipolar configuration: This is a combination of two monopolar in the sense that the two DC- lines can work independently in a situation where one line is out of service. It is commonly used for a HVDC application for an overhead transmission line.

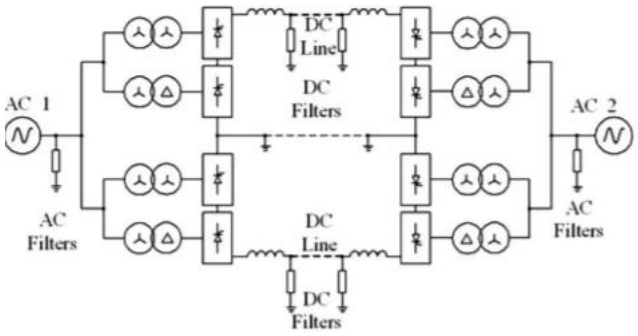


Figure 2-16: Bipolar CSC-HVDC system with one 12-pulse converter per pole [16]

ix. Multiterminal configuration: this is made up of more than two set of converters. The switching is done between the set of converters, converter 1 and 3 working as a rectifier while 2 works as an inverter. In the other way round, convert 2 working as a rectifier while converter 1 and 3 as inverter as shown in the figure below.

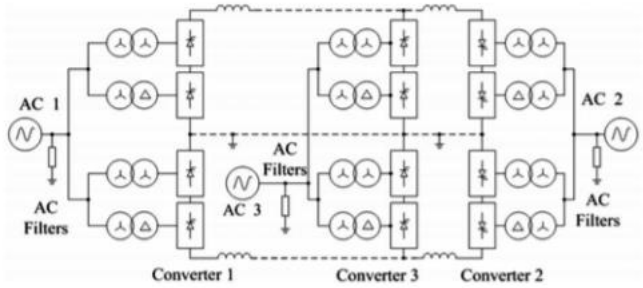


Figure 2-17: Multiterminal CSC-HVDC system—parallel connected [16].

### 2.9.2.2 CONVERTER COMPONENTS

For a clearer understanding of the HVDC system component especially in the converter stations, a single line diagram of a monopolar HVDC topology is shown in figure 2-18.

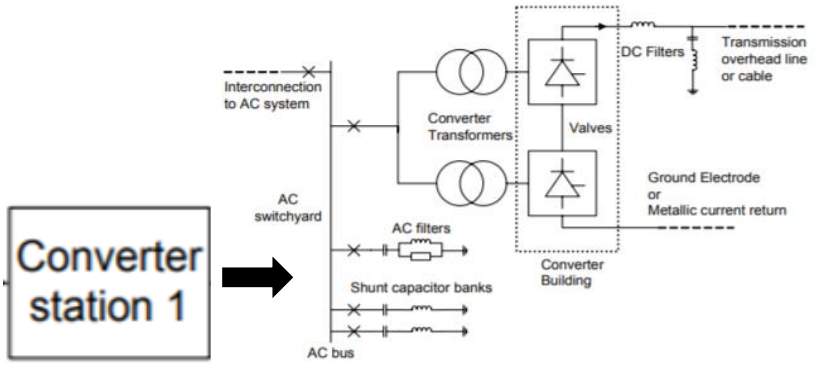


Figure 2-18: Single line diagram of a monopolar HVDC converter station [17].

From the above diagram, the converter station is made up of an AC switchyard which consist of the AC filters, shunt capacitor banks and the circuit breakers. The shunt capacitors compensate for the reactive power losses. Converter transformers systems (CTS) separated the AC from the Dc and brings down the voltage to an acceptable range for the valve's conversion process as the DC filters removes any leftover AC ripples from the DC current before it is transmitted by the DC-line.

### 2.9.2.3 THE AC FILTERS AND SHUNT CAPACITOR

The Ac filter reduces harmonics and frequency interference on the AC transmission line while the shunt capacitor serves as reactive power compensators.

### 2.9.2.4 The HVDC converter transformer system

Converter Transformers are important part of a HVDC converter as they are connected to the converter valves which is made up of twelve pulses to reducing the harmonics associated with the alternating current (AC) in a Y/Y/Δ $configuration$ [18]. The different configuration of the transformers is as shown in figure 2-19.

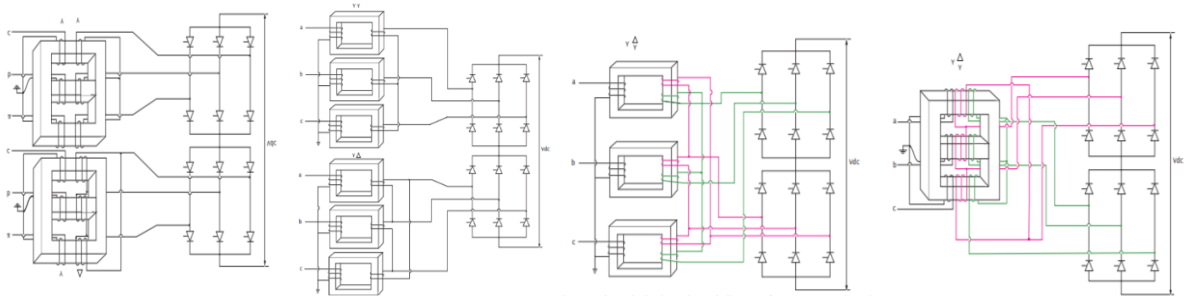

Figure 2-19: (a) Three phase two winding (b) single phase two winding (c) single phase three winding (d) three phase three winding [18]

#### 2.9.2.5 CONVERTER BUILDING

The converter building houses the converter made of either thyristors or transistor depending on the HVDC topology. Conversion of AC to DC and DC to AC takes place with the help of the converters. In the past as mentioned earlier the mercury arc valve were responsible for such conversion but the introduction of power electronics semi-conductors has led to the emergence of the Line commutated converter (LCC) and Voltage source converter (VSC)

## 2.10 HVDC TOPOLOGY

### 2.10.1 LCC-HVDC

In 1970, LCC-HVDC thyristor-based converter also known as current source converter CSC was first put in use in the HVDC transmission(96km,20MW) between Sweden and Island of Gotland. Afterwards, its use increased over the years as the first commercial HVDC in delivering up-to 1GW onshore and 500MW offshore over a distance not more than 100km.

#### 2.10.1.1 Components of LCC-HVDC Transmission system

The diagram below shows a typical LCC-HVDC system with the following components [19]

- PCC
- filters
- transformers bank
- Converters based on thyristor valves.
- Smoothing reactors.
- Capacitors banks or STATCOMs.
- DC cable and return path.
- Auxiliary power set.
- Protection and control devices.

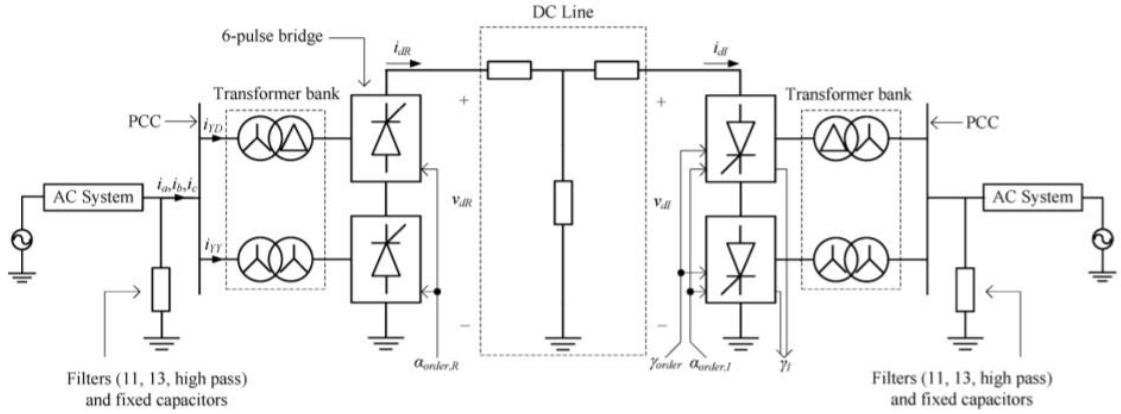


Figure 2-20: The 12-pulse LCC–HVDC system [19].

### 2.10.1.2 Thyristors

The main component of an LCC-converter is the thyristor, off which there will be no conversion of AC to DC and vice versa.

It is a silicon-based semiconductor made up of three terminals namely: Anode, cathode, and Gate. It has the capability of withstanding current of 4kA and voltage of 8kV. In other to increase its voltage capability, the thyristor will be connected in series [20]

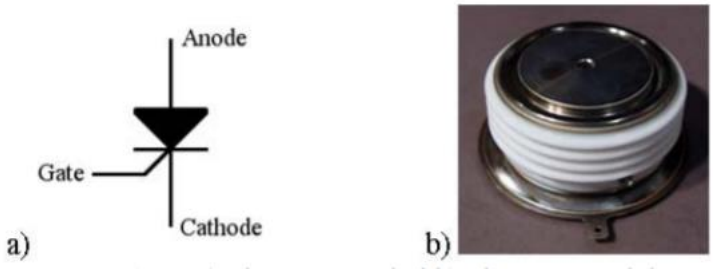


Figure 2-21: Thyristor

Graetz bridge configuration of the thyristor is a typical example of a thyristor arrangement in a three-phase power system consisting of six thyristors connected in series. Once the Graetz is turned on by a positive gate current, each of the thyristors conducts once in every half a cycle which is 60 degrees [21]. If the firing angle is less than 90 degrees, the thyristor performs the work of a rectifier but if greater than 90 degrees then it does the work of an inverter.

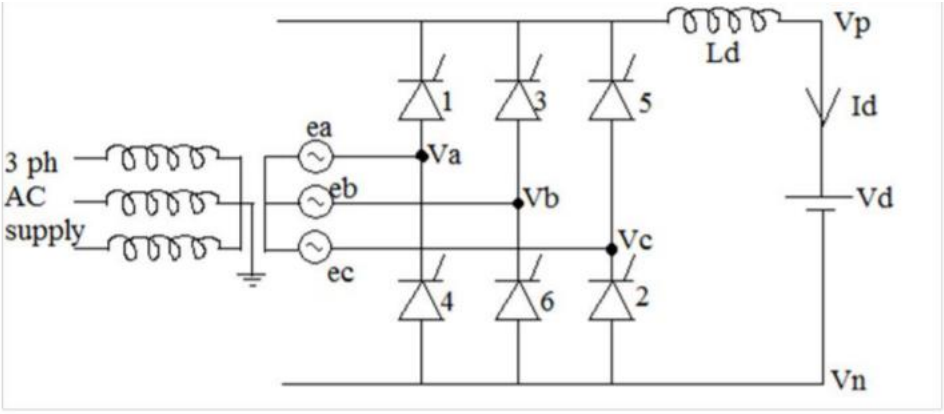


Figure 2-22: Graetz circuit

LCC-HVDC is said to be a current source converter because it requires a positive gate current for it to commutate and Dc current remains constant during the process.

## 2.10.2 VSC-HVDC Converter

Voltage source converter-HVDC is a semiconductor device that makes use of insulated gate bipolar transistor IGBT technology. This technology was first put in use in transmitting 50MW 80kVdc capacity of power in Gotland, Sweden in 1999.Due to its active and reactive power control, self-commutating which helps in black-starting a dead grid, VSC-HVDC is most commonly used in the integration of offshore wind farm to an onshore Ac grid[22].The figure below is a typical VSC-HVDC converter :

Voltage source converter-HVDC is a semiconductor device that makes use of insulated gate bipolar transistor IGBT technology. This technology was first put in use in transmitting 50MW 80kVdc capacity of power in Gotland, Sweden in 1999[22].Due to its active and reactive power control, self-commutating which helps in black-starting a dead grid, VSC-HVDC is most commonly used in the integration of offshore wind farm to an onshore Ac grid[23].

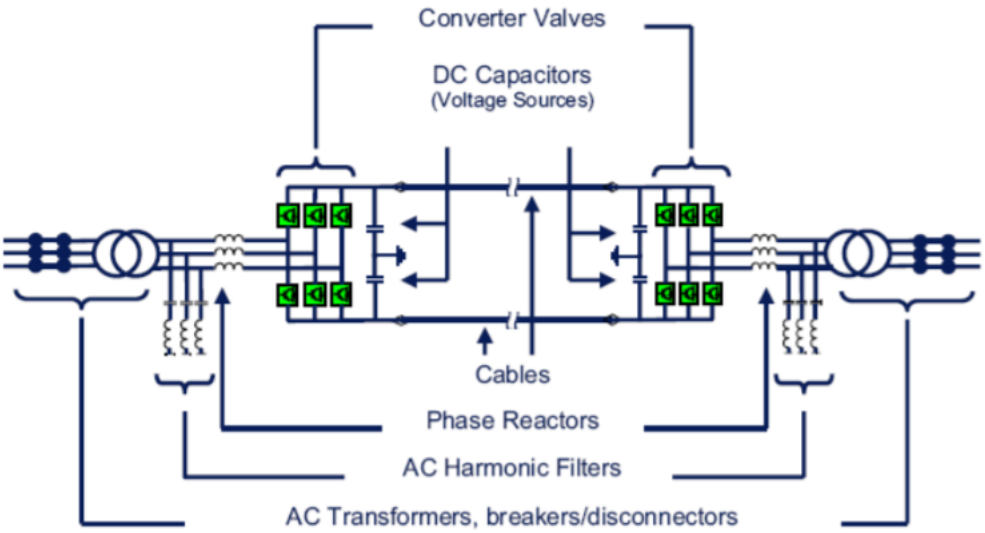


Figure 2-23: Simplified circuit diagram of a VSC HVDC [23].

A typical VSC-HVDC converter is made up of the following components:

i. Converter valves house the IGBT semiconductors and diode connected in parallel to IGBT as to create path for current flow.
ii. DC capacitors (voltage Sources) provides the stored energy required to control reactive and active power flow.it also helps to reduce the harmonics of the DC current.
iii. Phase reactors facilitates the transfer of active and reactive power from the AC system to the DC converter side.
iv. AC Harmonics filters does the work of reducing the harmonics of the converter outputs.

v. DC lines transmits direct current between the two converters stations. They are represented as a pi model of resistance, inductance and capacitance as shown in figure 2-24.

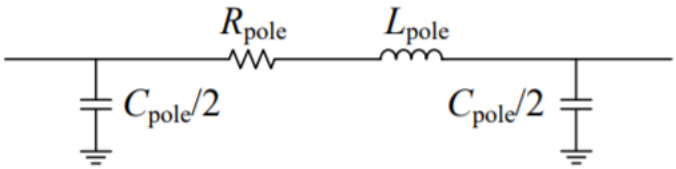


Figure 2-24: Pie model of a single pole for a dc-transmission link

vi. AC transformer

### 2.10.2.1 Insulator-Gate Bipolar Transistor (IGBT)

IGBT is a semiconductor device used in VSC-HVDC for switching of current from AC to DC and vice versa using pulse width modulation. The combination of BJT and MOSFET makes the semiconductor device suitable for high commutation and low conduction losses. IGBT is made of three terminals- collector, emitter and gate, a small voltage value at the gate can conduct current up to 2.4kA and block voltage of about 6.4kV. The semiconductor conducts when voltage across the gate and emitter ($V_{GE}$) is higher than the threshold voltage $V_{GE(TH)}$to be in an active region and in cut off region once the gate voltage is removed and Increase in the gate voltage increases the conducting current as represented in the figure 2-25.

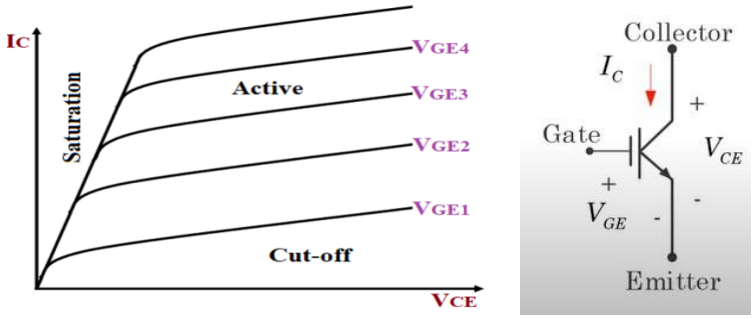


Figure 2-25: (a) VI Characteristics (b) Symbol

Switching capability of the IGBT semiconductor is achieved by the Pulse width modulation technology.

### 2.10.2.2 PULSE WIDTH MODULATION

Pulse with modulation is used to control the average output voltage by varying the width of the input pulse. VSC-HVDC converter has a faster and quick response in dynamics due to the pulse width modulation technique of the IGBT.

Generation of pulse width modulated signal is produced by comparing the input sinusoidal signal with the sawtooth triangle signal using a comparator [24].

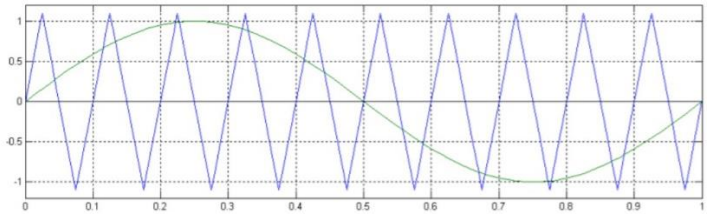

Figure 2-26: PWM switching signal

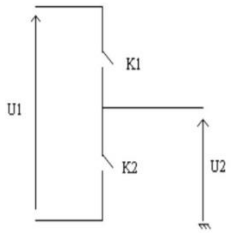


Figure 2-27: Basic circuit for PWM

Switch K1conducts if the value of the sinusoidal waveform is higher than the triangular wave and U2 =U1 but if otherwise, U2= -U1 to give the output waveform as shown in figure 2-28.

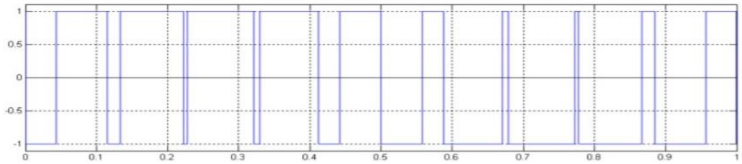

Figure 2-28: Output Waveform of PWM

The amplitude of the modulation is given in equation 22

$$m_a = \frac{\hat{V}_{sin\ control}}{\hat{V}_{tri}} \tag{22}$$

Where,

$\hat{V}_{sin\ control}$is the peak amplitude of the sinusoidal control voltage

$\hat{V}_{tri}$ is the peak amplitude of the triangular voltage which is constant

## 2.11 Quasi Steady State

### 2.11.1 Definition and Basic Principle

Quasi steady state is a situation that is changing slowly enough that it can be considered as constant. It acts like a middle ground for transient and steady state model where there are two approaches, either to look at just the voltage or the active/reactive power.

The use of P-V curves in quasi-steady state analysis can effectively demonstrate various factors influencing the voltage stability of a power system. The goal of this paper is to show how quasi steady state analysis can be used to better understand dynamic voltage stability. Quasi steady state analysis using P-V curves is a useful learning tool because it allows you to visualize the causes and effects of a power system's voltage stability without having to run a time domain simulation. It also allows for the visualization of potential voltage collapse locations and the determination of how close a power system is to voltage collapse. [27]

Because of the difference in the phenomena to be researched and the difference in time scale, an electromagnetic model cannot be utilized directly for electromechanical dynamic analysis. As a result, a quasi-steady-state model of the VSC-HVDC transmission system is required to capture the dynamics of the VSC-HVDC for large AC/DC system electromechanical modelling.

The components of the VSC-HVDC Voltage Source Converter comprise a three-phase full-controlled converter bridge, converter reactor, DC capacitor, and AC filter. The active and reactive power that the converter exchanges with the ac system, ignoring the harmonic component, are stated as:

$$P = \frac{U_S U_C}{X} sin\delta \quad (23)$$

$$Q = \frac{U_S(U_S - U_C cos\delta)}{X} \quad (24)$$

Where $U_s$ is the line-to-line fundamental voltage of the AC bus., $U_c$ is the converter bridge output line-to-line ac fundamental voltage, δ refers to the angle $U_c$ lag $U_s$, X is the value of the converter reactor L.

From expression (23), active power and its direction mainly depend on δ, the direction of direct current and the magnitude of active power could be controlled by controlling δ.

From expression (24), the reactive power transmission mainly depends on ($U_s$ – $U_c$ cosδ), we can control reactive power of VSC by controlling the magnitude of $U_c$.[28]

The magnitude of active and reactive power, as well as the direction of transmission, can be controlled in the VSC-HVDC system using PWM technology by controlling the phase and magnitude modulation ratio of the SPWM, allowing the active and reactive power to be regulated at the same time and independently. The magnitude modulation ratio M and the shifted phase compared to the ac bus voltage are two control variables for the voltage source converter that uses PWM technology. The fundamental component of the output AC voltage is as follows:

$$U_c = \frac{\mu M}{\sqrt{2}} u_d \angle \delta \tag{25}$$

Where $u_d$ refers to DC voltage; μ refers to the utilization of
DC voltage related with the PWM mode. At ac side, VSC could be equivalent to an ideal synchronous generator, its magnitude and phase angle could be controlled. [28]

### 2.11.2 QSS Model of VSC-HVDC Link

Each synchronous machine is characterized by three variables:

$E_q$ – the emf proportional to field current

$E_q^s$ – the corresponding emf behind saturated synchronous reactances

$\varphi$ – the internal rotor (or load) angle

These variables are involved in three algebraic equations [35]:

Machine saturation

$$E_q - k\left(E_q, E_q^s, \varphi, V\right)E_q^s = 0, \qquad k > 1 \tag{26}$$

Voltage regulation by AVR

$$E_q - G(V^0 - V) = 0 \tag{27}$$

Speed regulation

$$P - P^m = P\left(E_q, E_q^s, \varphi, V\right) - P^0 + \alpha_g \omega \tag{28}$$

Where,

P – active power

$P_m$ – turbine mechanical power

$P_0$ – power setpoint

V – voltage

$V^0$ – voltage setpoint

G – open-loop steady-state gain of the AVR

$\alpha_g$ – participation factor, function of the permanent speed droop and turbine rating

The sensitivity of load power to voltage and frequency through the exponential model is [30]:

$$P = P^0(1+\omega)^{\gamma} \sum_{j=1}^{3} a_j \left(\frac{V}{V^0}\right)^{a_j} \tag{29}$$

$$Q = Q^0(1+\omega)^{\delta} \sum_{j=1}^{3} \beta_j \left(\frac{V}{V^0}\right)^{\beta_j} \tag{30}$$

A point-to-point VSC-HVDC link connects a wind farm with doubly fed induction generators (DFIGs) to an onshore ac grid. The wind farm VSC (WFVSC) controls the amplitude and frequency of the WFVSC ac terminal voltage to enable wind power collection in the VSC-HVDC link. The grid side VSC (GSVSC) maintains a consistent dc link voltage and offers reactive power assistance to the onshore ac grid to keep the PCC voltage at a predictable level. To accomplish separate control of active and reactive power, the d, q-axis decoupling current controller is employed.[29]

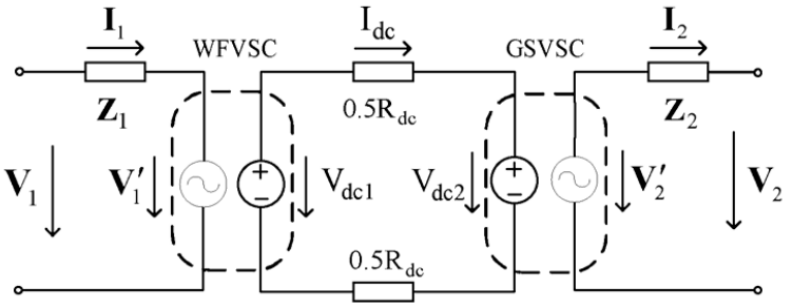


Figure 2-29: QSS model of point-to-point VSC-HVDC link [29]

Figure 2-29 shows the QSS model of the point-to-point VSC-HVDC link where $\mathbf{V_1}$ is the voltage phasor of WFVSC ac terminal, $\mathbf{V_2}$ is the voltage phasor of GSVSC ac terminal, $\mathbf{V'_1}$ is the AC side voltage phasor of WFVSC, $\mathbf{V'_2}$ is the AC side voltage phasor of GSVSC, $V_{dc1}$ is the DC side voltage of WFVSC, $V_{dc2}$ is the DC side voltage of GSVSC, $\mathbf{I_1}$ is the AC side current phasor of WFVSC, $\mathbf{I_1}$ is the AC side current phasor of GSVSC, $I_{dc}$ is the DC link current, $\mathbf{Z_1}$ is the sum of WFVSC commutating reactor impedance and equivalent impedance of switch losses, $\mathbf{Z_2}$ is the sum of GSVSC commutating reactor impedance and equivalent impedance of switch losses and $R_{dc}$ is the resistance of dc cables.

VSCs can quickly alter the amplitude and phase angle of their ac side voltage using PWM technology to achieve separate control of active and reactive power. As a result, VSCs may be modelled as regulated voltage sources for ac grid stability study. The usual reaction time of dc dynamics in VSC-HVDC systems (in the range of milliseconds) is significantly faster than the time scale of long-term stability. As a result, in the proposed HVDC QSS model, rapid dc dynamics are approximated by their equilibrium conditions. DC capacitors are the same as voltage sources since their steady-state voltages are the same. The inductance of a dc cable is usually ignored since it is small.

The AC side voltage phasor of WFVSC and GSVSC and the DC side voltage of WFVSC and GSVSC has the following relations:

$$V'_1 = \frac{M_1}{\sqrt{2}} V_{dc1}, \qquad V'_2 = \frac{M_2}{\sqrt{2}} V_{dc2} \tag{31}$$

where the symbols of and indicate the PWM modulation ratios of the WFVSC and GSVSC, respectively. [29]

## 2.12 Voltage Instability Detection

### 2.12.1 Power System Stability

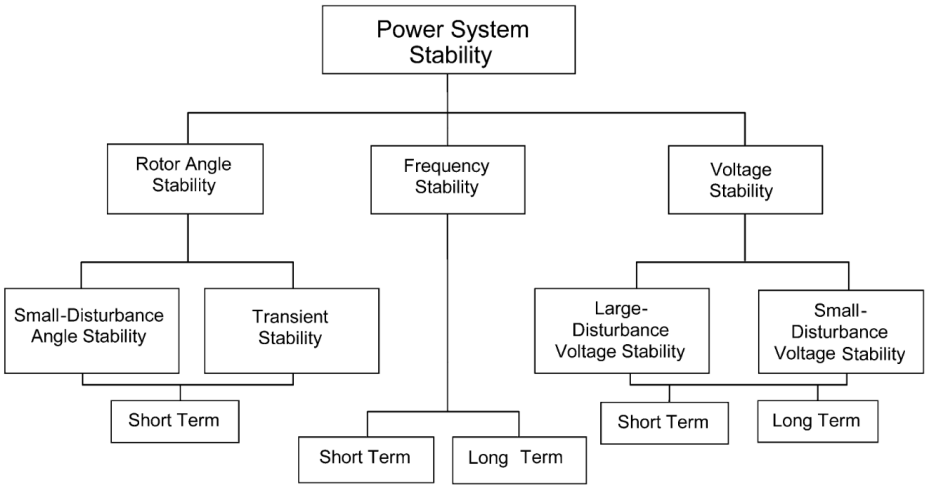


Figure 2-30: Classification of Power System Stability [25]

Voltage stability is a subsection of power system stability as shown in Fig. 2-30

The definition of voltage stability is given by the IEEE/CIGRE Join Task Force [25]. "Voltage stability is the ability of a power system to maintain steady, acceptable voltages at all buses in the system under normal operating conditions and after being subjected to a disturbance."

Further voltage stability is categorized into the following subcategories:

1. **Large-disturbance voltage stability** is the capacity of a system to sustain stable voltages in the face of major disruptions like as system failures, loss of generation, or circuit contingencies. The time span of interest for research might range from a few seconds to tens of minutes.

2. **Small-disturbance voltage stability** is the capacity of a system to sustain stable voltages in the face of minor disturbances, such as gradual changes in system load. The features of loads, continuous controls, and discrete controls at a particular instant of time impact this type of stability. This idea is important in determining how the system voltages will respond to modest system changes at any given time.

3. **Short-term voltage stability:** The dynamics of fast-acting load components such as induction motors, electronically controlled loads, and HVDC converters have a role in short-term voltage stability. The study time is a few seconds long, and analysis necessitates the solution of appropriate system differential equations.

4. **Long-term voltage stability:** Longer-acting equipment, such as tap-changing transformers, thermostatically regulated loads, and generator current limiters, are used to provide long-term voltage stability. Long-term simulations are necessary for examination of system dynamic performance when the research period of interest is several or many minutes. [26]

## 2.12.2 Thevenin Equivalent of an HVDC-Connected Offshore Wind Farm

### 2.12.2.1 Thevenin Equivalent

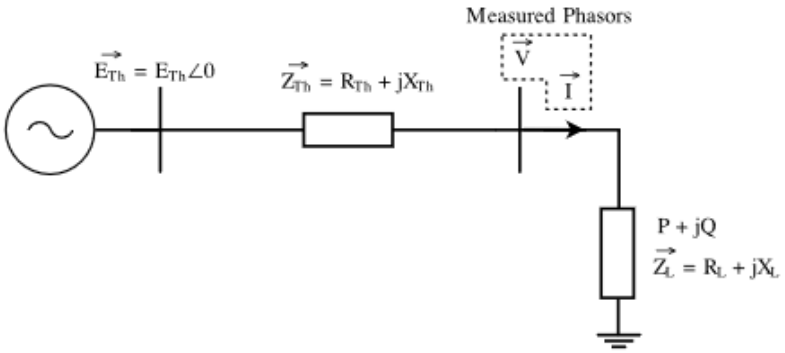


Figure 2-31: Thevenin equivalent circuit [31]

Fig 2-31 show the classic Thevenin equivalent circuit which consists of voltage $\vec{E}_{Th} = \vec{V} + \vec{I}\vec{Z}_{Th}$, impedance $\vec{Z}_{Th}$, local measured phasors of voltage $\vec{V}$ and current $\vec{I}$ as seen from the load bus with impedance $\vec{Z}_L$. Here, the voltage stability issues are estimated bus the indicator ISI (Impedance Stability Index) which indicates that the closer the load demand is to the estimated load impedance magnitude, the more likely it is to have voltage issues which means if the load impedance is larger than the Thevenin impedance the system is considered as stable and given by the formula [33].

$$ISI = \frac{|\vec{Z}_{Th}|}{|\vec{Z}_L|} \tag{32}$$

If the magnitude of the load impedance is considered equal to the magnitude of Thevenin impedance then the maximum power transfer can be estimated as,

$$S_{Max} = \frac{E_{Th}^2[Z_{Th} - (I_m(\vec{Z}_{Th})sin\varphi + Re(\vec{Z}_{Th})cos\varphi]}{2[Im(\vec{Z}_{Th})cos\varphi - Re(\vec{Z}_{Th})sin\varphi]^2} \tag{33}$$

Voltage collapse can occur if the maximum loadability is crossed, differing on the load characteristics which can be nonlinear and dynamic with a load recovery characteristic. Hence, maximum power transfer is considered for the voltage stability limit and the power margin can be given as the difference between the maximum power transfer and the apparent load power [34].

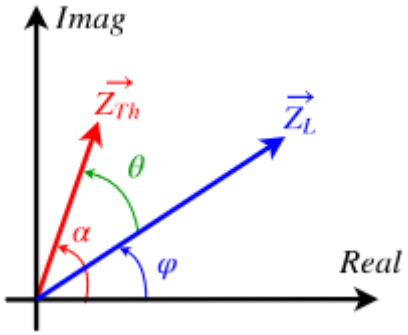


Figure 2-32: Phase difference between load and Thevenin impedance

The angle of Thevenin impedance can be given as $tan^{-1}\frac{X_{Th}}{R_{Th}} = \alpha$ where, $\alpha = \theta + \varphi$ and $X_{Th}$ and $R_{th}$ are the Thevenin reactance and resistance. An X/R ratio can be adjusted using angle as a setting parameter and the incorrect ratio can lead to a large error in the estimation of the Thevenin impedance [32].

### 2.12.2.2 HVDC-connected Offshore wind farm

This project uses a DFIG equipped wind turbine where wind turbine is connected to two PWM inverters back-to-back via slip ring which are thus connected to the AC/grid network via step-down transformer. Both the PWM inverters has IGBT, the magnitude and the direction of the power flow between the rotor circuit and the supply can be controlled by the IGBT switches [11].

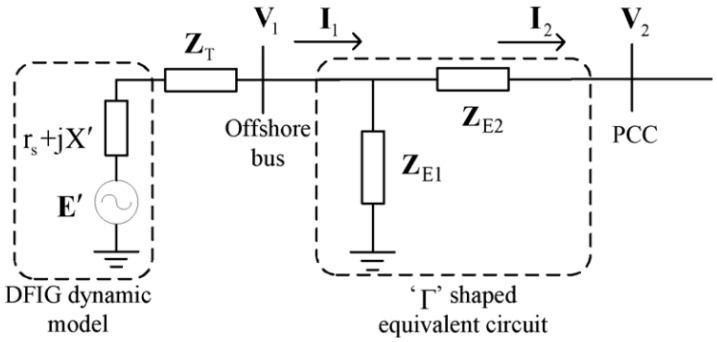


Figure 2-33: Equivalent circuit of an HVDC-connected offshore wind farm [29]

HVDC-connected offshore wind farm can be modelled using the 'T' shaped equivalent model as shown in figure 2-33 with the DFIG is represented by the dynamic model of an integrated generator where the $r_s$ is the stator resistance and X' transient reactance which is given by

$$X' = \omega_s \frac{L_{ss} - L_m^2}{L_{rr}} \tag{34}$$

Where, $L_{ss}$ and $L_{rr}$ are the self-inductance of stator and rotor windings, $L_m$ is the mutual inductance between them and $\omega_s$is the synchronous speed.

### 2.12.3 Voltage Instability Detection

From figure 2-23, the equivalent impedances are

$$Z_{E1} = \frac{V_1}{I_1 - I_2} \tag{35}$$

$$Z_{E2} = \frac{V_1 - V_2}{I_2} \tag{36}$$

PMU measurements at the VSC ac terminals as shown in Figure 2-31 can be used to formulated into Thevenin equivalent impedance as [29]

$$Z_{th} = \frac{(r_s + jX' + Z_T) * Z_{E1}}{r_s + jX' + Z_T + Z_{E1}} + Z_{E2} \tag{37}$$

The magnitude of $Z_{E1}$ is much larger than the magnitude of $Z_{E2}$ before the voltage collapse. So, the Thevenin impedance mainly depends on the HVDC equivalent parameter $Z_{E2}$ i.e.,

$$Z_{th} = Z_{E2} = \frac{V_1 - V_2}{I_2} \tag{38}$$

$Z_{load}$is the load impedance which can be observed at the PCC as lumped load and it can be calculated as

$$Z_{load} = \frac{V_2}{I_2} \tag{39}$$

It can be said from the equation 33 that during the system operation, the maximal power transfer of a power grid corresponds to the point of voltage collapse. Therefore, the difference between the load and Thevenin impedance magnitudes, i.e., $|Z_L| - |Z_{Th}|$ can be used to determine the proximity of the operating point to a voltage collapse, i.e., a voltage stability margin.

# 3 Network Definition in DIgSILENT Power Factory

This chapter discusses the modelling of an HVDC link for a 400 MW offshore wind farm consisting of DFIG wind turbines. Voltage source converters (VSC) are used in the Grid Side and Wind Farm of the HVDC connection. The load flow calculation and time-domain simulation are covered in this simulation. DIgSILENT PowerFactory and MATLAB are used to analysis the different perspective of the project, but main part of the simulation is done in PowerFactory. The PowerFactory has already some standard projects in example section. So, for simulation HVDC, Offshore windfarm, and IEEE-9 bus system are integrated with each other. The system description of all the components is described below.

## 3.1 VSC-HVDC Transmission System

The HVDC consists of two voltage source converter, HVDC transmission lines, and local three phase step up transformer on the onshore grid side. The network consists of two parts one is offshore and second is onshore. The AC offshore is directly connected with the Voltage source converter on the offshore side and then with the help of HVDC transmission lines connected with voltage source converter on the onshore side. The onshore VSC is attached with on shore transformer. The network is shown below in figure 3-1. [36]

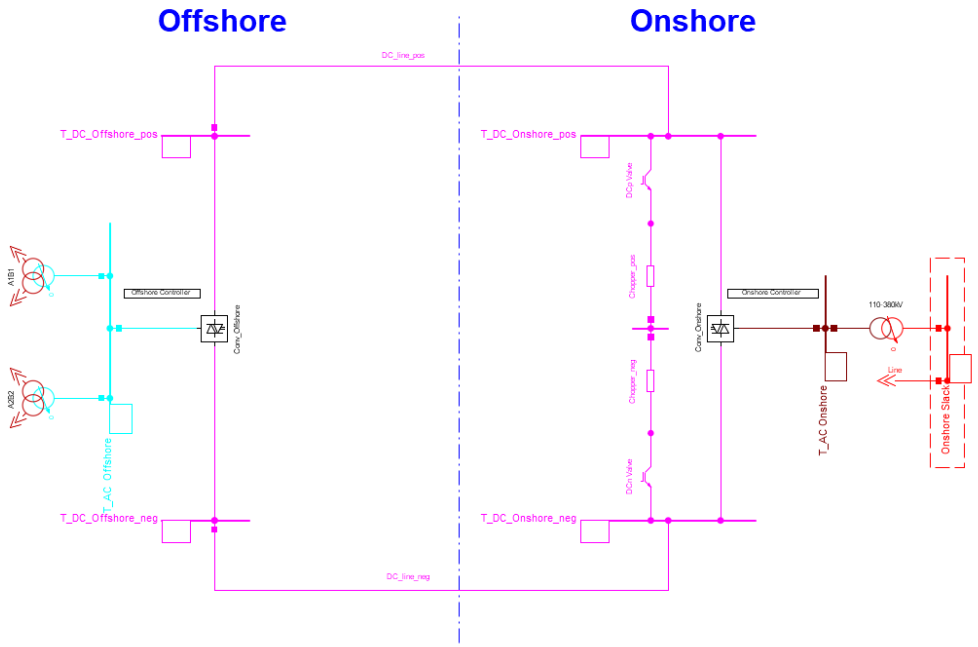


Figure 3-1: PowerFactory model of VSC-HVDC line

There are two 3-winding transformer which connects offshore wind farm to HVDC line, and the parameters of the type used in PowerFactory is detailed in table 2.

All parameters of the voltage source converter is presented with the help of table 3.

The parameters for the high voltage DC transmission lines are mentioned below in the table 4.

The basic data of the onshore transformer is mentioned in table 5.

## 3.2 DFIG Wind Farm

The simulated model is 400 MW offshore wind farm consisting of DFIG dynamic model that includes the wind turbine, induction generator, power electronic dc link, control system, and DFIG protection circuit. There are 80 standard DFIG each rated at 5MW which are connected to the collector bus through step up transformer. Among 80 only 10 of the turbines are modelled as individual machines and 70 are aggregated into four DFIG models. Fig 3-2 shows the PowerFactory model of DFIG wind farm which consists of 70 wind turbines, 4 step up transformers, 4 neutral earthing compensators (NEC) connected at four buses, 2 three phase transformers connected to AC Offshore bus which is thus connected to VSC-HVDC link. [36]

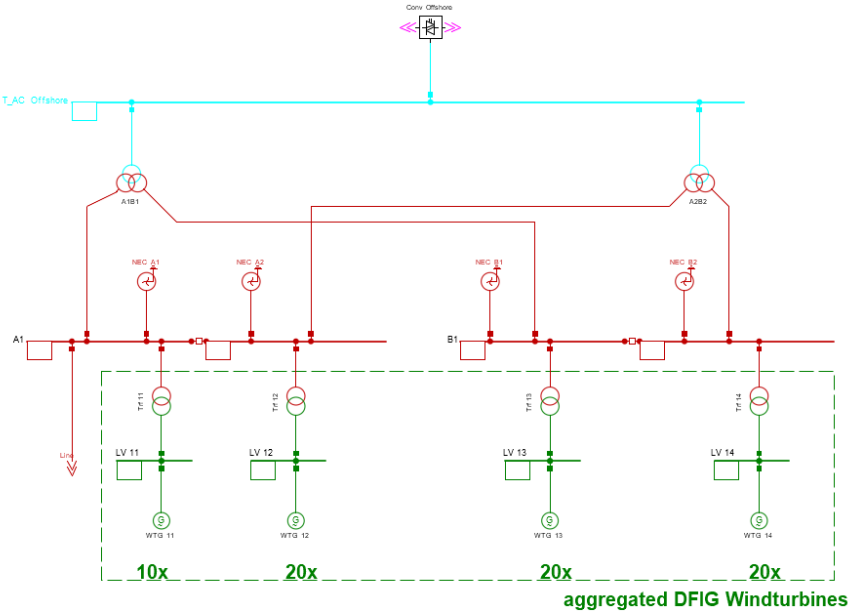


Figure 3-2: PowerFactory Model of DFIG Wind Farm

Figure 3-3 shows the detailed feeder consisting of 10 DFIG out of 80 model which has the parameters shown in table 1 with 10 transformers which has the parameters shown in table 7.

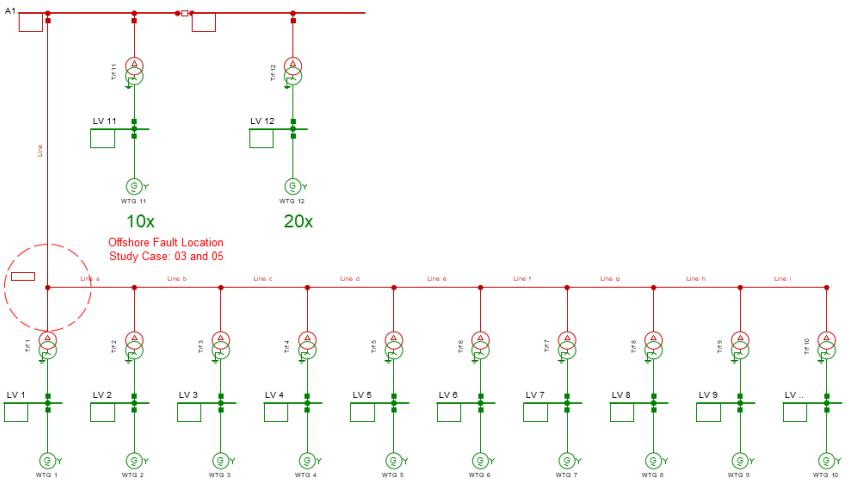


Figure 3-3: Detailed Feeder for 10 DFIGs

All the DFIG wind turbine has been model with same model type, the parameter of the type is listed in table 6.

First set of DFIG consists of 10 parallel machines, second set consists of 20 parallel machines rated, third set consists of 20 parallel machines and last set consists of 20 parallel machines making it a total of 70 machines which are connected to their relative buses having voltages 0.69 kV which is then connected to 2-winding step up transformer, the parameter of the transformer type is listed in table 2.

All these four transformers are connected to four different busbar each with line-line nominal bus voltage of 33 kV. Four neutral earthing compensators (NEC) are connected to these four busbars which parameters are listed in table 8.

These four buses are connected to 3-winding transformer of and thus to AC Offshore busbar whose parameters are given in chapter 3.1.

Busbar A1 has internal switches and circuit breakers for the protection of DFIG which is connected via a sea cable line of length 1.5, rated 1 kA current and 33 kV voltage, with resistance 0.0387 Ohm/km, reactance 0.103672 Ohm/km and susceptance 94.24778 µS/km, as shown in figure 3-4.

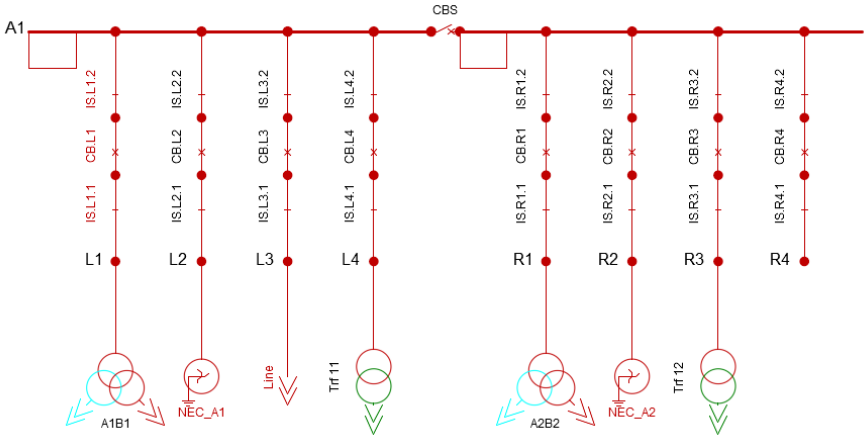


Figure 3-4: Single Busbar with Tie

## 3.3 9 Bus System

The simulated model has the IEEE 9 Bus system connected as a grid connected to onshore slack bus which is considered a load. The system consists of 9 buses, 3 generators, 3 loads, 6 lines and 3 transformers. [37]

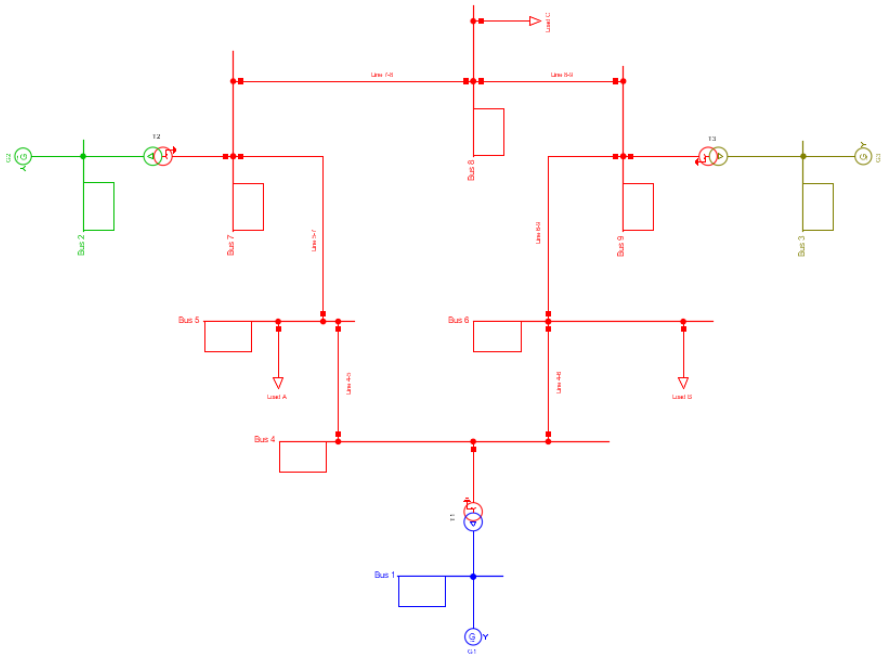

Figure 3-5: Single line diagram of the Nine-bus System

The nominal voltage of the transmission system is 230 kV, and the nominal frequency is 60 Hz. The line-line nominal voltages of all the buses are given in table 9.

Three generators are connected to bus 1,2 and 3 respectively. The parameters of the generator type are given in table 10.

The three loads are connected in bus5,6 and 8 respectively. The parameters of the load with 100 MVA base are given in table 11.

There are total of six lines connecting 6 buses (bus 4 to bus 9) with their own types which are listed in table 12 where the first number of lines indicates From-Bus and last number indicated To-Bus.

There are total of three transformers between six buses which are described in table 13.

# 4 Simulations and results

In this chapter, all the simulations done in the DIgSILENT PowerFactory are discussed. There are two stages in the simulations, the first stage is combining two inbuilt PowerFactory projects, make it run smooth, with load flow calculations, voltage profiles and which is done by using the merge tool in the PowerFactory and with following steps:

1. Load the two example projects “Offshore Wind Farm” and “9 Bus System” from the PowerFactory Examples.
2. Right click on “Offshore Wind Farm” and choose the command ‘Select as Base to Compare’.
3. Right click on “9 Bus System” and choose the command ‘Compare to Base Project Name’.
4. The Compare and Merge Tool command will be shown. Select the option Manually → Into → Base and click on execute.
5. Initially assign all data from 1st to Base
6. Multi-select all items having the ‘+’ sign in the Base column, right click and choose Assign with children from →Base
7. Repeat step 8 for the folders Library/Operational Library, Library/Scripts, Library/Templates, Library/User Defined Models, Network Model/Diagrams, Network Model/Diagrams, Network Data, Network Data/Variations, Network Data/Areas, Network Data/Boundaries, Network Data/Paths, Network Data/Zones, Operation Scenarios, Study Cases, Settings, and any other project folders that may contain information from the Base project.
8. Click on Check button and observe the errors (if any) being shown in the output window. After all referencing errors have been solved, click on ‘Merge’.
9. Activate the “Offshore Wind Farm” project. It contains all information from both projects.
10. To connect two projects in single line diagram, a ‘Line’ is created between ‘Onshore Slack Bus’ in ‘HVDC’ and ‘Bus 9’ in ‘Nine-bus System’ with drag and drop method between two single line graphic pages.

All the thirteen study cases from both the projects are loaded but the simulation work is only done in Base_Case which contains all the four grids namely ‘150-33kV Offshore Station’, ‘HVDC’, ‘Nine-bus System’, and ‘Windpark’. The load flow calculations are then carried out which is shown in figure 4-1.

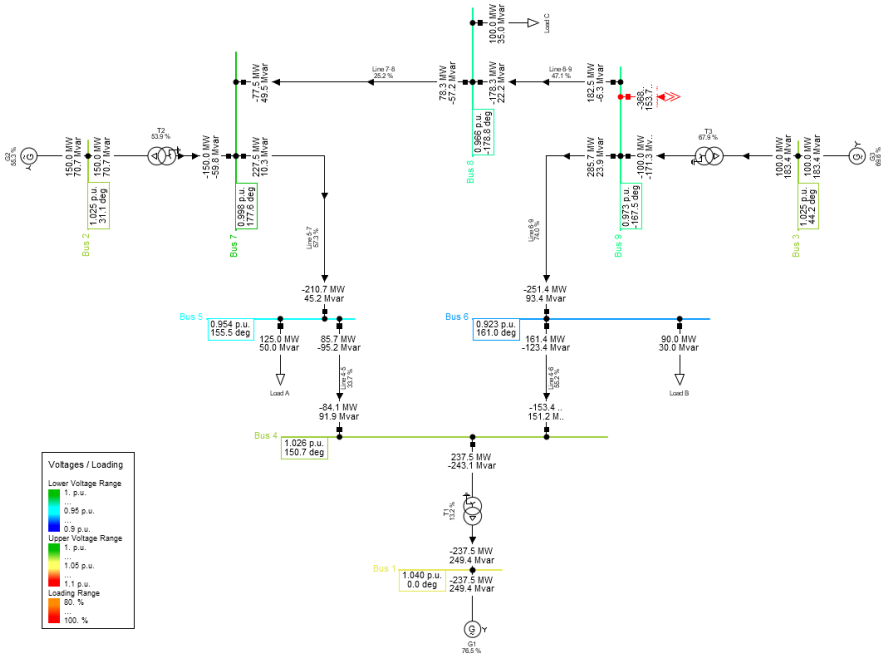


Figure 4-1: Load flow calculations on 9 bus system

In mode ‘Simulation RMS/EMT’ the initial conditions are checked, and RMS/EMT simulation is run for 15 seconds. The voltage profile of all nine buses along with onshore slack buses are plotted which is shown in figure 4-2.

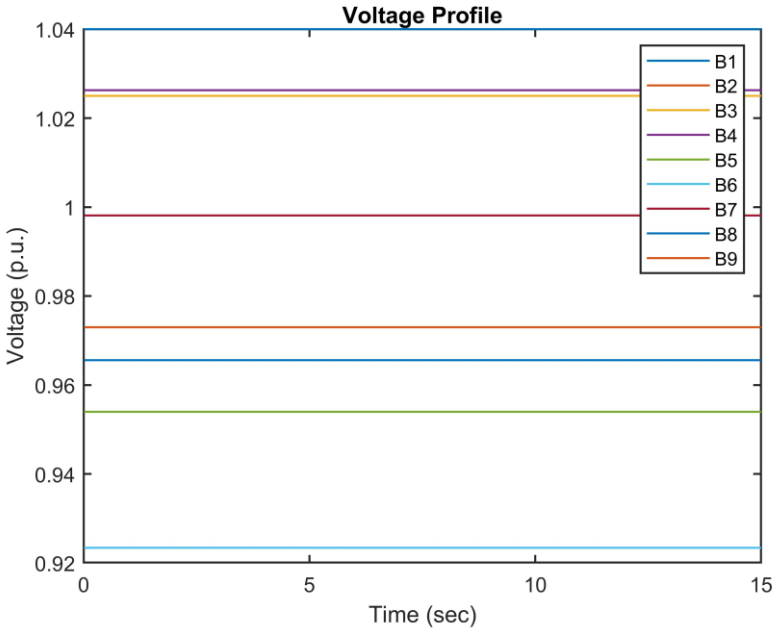


Figure 4-2: Voltage Profile

From figure 4-1 & 4-2, it is seen that the merge project works well with load-flow calculation and RMS/EMT simulation and the whole system is in steady-state condition with constant voltage across HVDC and 9 bus system.

In the second phase of the simulation, the events are added, and the voltage stability is detected. For this, we start with the creation of events as shown in Table 14.

Table 2: Event list of cascading failures

| Lines | Time | Events |
|---|---|---|
| Line 8-9 | 5 s | Initiate a three-phase short circuit fault |
| Line 8-9 | 5.15 s | Clear short circuit fault |
| Line 7-8 | 10 s | Overloaded and Isolated |

After adding all these events, the simulation RMS/EMT is run for 15 seconds and voltage of bus 8,9 and Onshore slack bus is plotted for instability studies.

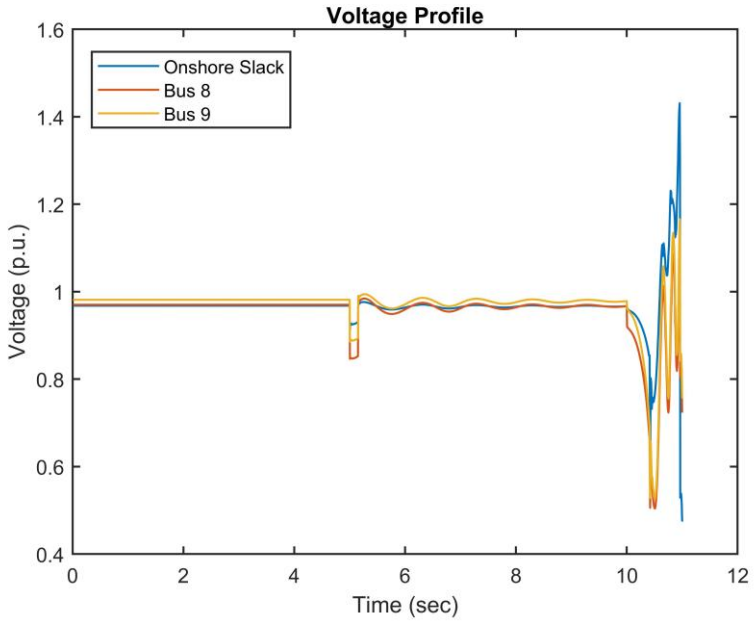


Figure 4-3: Voltage profile after events

From figure 4-3, it is seen that when the three-phase short circuit is added at 5 seconds, the voltage drops quite significantly since the fault current is proportionally larger than rated current and as soon as the fault is clear at 5.15 seconds, the voltages rise back up again to the rated bus voltages and there are some oscillations for few seconds before it comes back to completely steady again.

The line 7-8 is overloaded by decreasing it's rated current to its half and at 10 seconds, the isolation event is added which results in complete voltage collapse within 0.56 seconds. As power transfer increases, more reactive power is needed to keep the voltage at the expected level. When the generator unit runs out of reactive power reserve, the PV node behaves like a PQ node. The resulting voltage drop worsens the power shortage and leads to a voltage collapse.

The VSC-HVDC system combined with offshore windfarm accommodates Thevenin circuits with PCC/Onshore Slack bus as a virtual load bus. Both VSC stations of HVDC are expected to be equipped with a PMU for real-time measurement of voltage and current vectors at the AC terminals. The voltage and current pointers on the VSC-AC terminals during the simulation with DIgSILENT are transferred to MATLAB to identify the Thevenin and load impedance displayed in real time. Detection of voltage instability is achieved by comparing the impedance of the synchronized load and Thevenin.

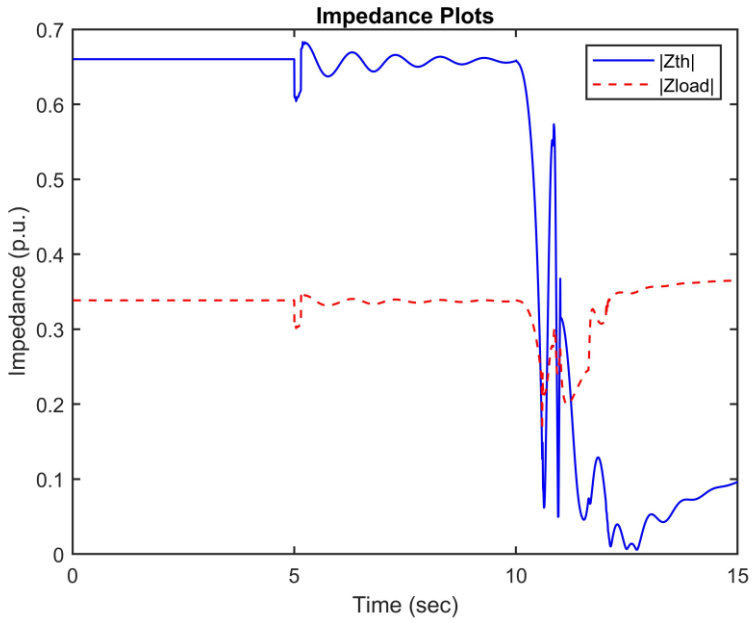


Figure 4-4: Thevenin vs load Impedance

Figures 4-4 shows the equivalent Thevenin, and load impedance magnitudes viewed at PCC. From the graph, it is seen that both the impedances decrease at 5 sec when there is three phase fault and then comes back to normal after three-phase fault has been cleared at 5.15 sec which was same cases for the voltage profiles. When the third event comes into action after 10 sec, the figure shows the Thevenin impedance and load impedance falls exactly at 10.56 sec when the voltage had collapsed, the impedances cross each other, which is a clear indication of the real dynamics of HVDC system operation.

# 5 Summary

## 5.1 Conclusion

The main goal of this project is to use DIgSILENT PowerFactory to model a VSC-HVDC and wind farm for a voltage stability study based on circuit theory. The phasor measuring unit (PMU) measures power system phasor values in real time for online voltage instability analysis using Thevenin's impedance matching.

The voltage source converter-based high voltage direct current (VSC-HVDC) technology allows large-scale offshore wind farms to be linked with onshore ac grids. The impact on the security of ac grids as a result can be severe. As a result, developing an HVDC model for online stability monitoring of integrated ac/dc systems is critical. The HVDC equivalent circuit allows the PMU data to be used to establish the Thevenin equivalent impedance of an HVDC-connected offshore wind farm.

The two inbuilt PowerFactory example projects “Offshore Windfarm” and “9 Bus System” are merged together. Three cascaded events are added to analyse the voltage and current phasors for instability analysis. The voltages and current plots were as exported to MATLAB to calculate the Thevenin and load impedance in order to find the difference in magnitude for voltage stability margin.

The testing networks are built in the PF, and several relevant simulations are performed to reach the objective. Simulations in the Offshore Windfarm, HVDC and 9 Bus System show that in PowerFactory they are able to exhibit voltage stability analysis. The simulations in the integrated networks are performed to analyse the capability of the grid to integrate offshore wind farm. It is seen that the overloading and isolation of any bus in the 9 bus system could lead to voltage collapse of the power system.

## 5.2 Future Work

This project presents the detailed simulation of voltage instability detection when the VSC-HVDC connected offshore windfarm is connected to 9 Bus System, so there can be unlimited amount of research work in the future considering this project as a base, some of which are listed below:

1. Load shedding for voltage collapse mitigation

   Load shedding can be activated at 10.4 sec i.e., when the voltage collapses, to increase the voltage stability margin and restore the system voltage.
2. Short-term instability studies

   The proposed HVDC model is not intended for short-term instability studies which can be considered as future research studies.
3. Implementation of real grid

This project focuses on standard 9 Bus system which can be replaced with real grid for e.g., Nordic grid, to analyse the potential offshore wind farm integration in the future.

4. Quasi-Dynamic Simulation
   This project focuses on RMS/EMT simulation, but the future work can be Quasi-Dynamic simulation for 24 hours' time, which can be done by importing real time characteristic of load (9 bus system).

# Reference


[1] G. M. Joselin Herbert, S. Iniyan, E. Sreevalsan, and S. Rajapandian, 'A review of wind energy technologies', *Renew. Sustain. Energy Rev.*, vol. 11, no. 6, pp. 1117–1145, Aug. 2007, doi: 10.1016/j.rser.2005.08.004

[2] A. Sarkar and D. K. Behera, 'Wind Turbine Blade Efficiency and Power Calculation with Electrical Analogy', vol. 2, no. 2, p. 5, 2012

[3] T. Haugsten Hansen, 'Offshore Wind Farm Layouts: Performance Comparison for a 540 MW Offshore Wind Farm', 235, 2009, Accessed: Nov. 15, 2021. [Online]. Available: https://ntnuopen.ntnu.no/ntnu-xmlui/handle/11250/256657

[4] P. Bresesti, W. L. Kling, R. L. Hendriks, and R. Vailati, 'HVDC Connection of Offshore Wind Farms to the Transmission System', IEEE Trans. Energy Convers., vol. 22, no. 1, pp. 37–43, Mar. 2007, doi: 10.1109/TEC.2006.889624

[5] P. Nanda, C. K. Panigrahi, and A. Dasgupta, 'Phasor Estimation and Modelling Techniques of PMU- A Review', Energy Procedia, vol. 109, pp. 64–77, Mar. 2017, doi: 10.1016/j.egypro.2017.03.052

[6] D. Hart, D. Uy, V. Gharpure, D. Novosel, D. Karlsson, and M. Kaba, 'PMUs- a new approach to power network monitoring', Jan. 2001

[7] R. P. Haridas, 'Synchrophasor Measurement Technology in Electrical Power system', Int. J. Eng. Res., vol. 2, no. 6, p. 6, 2013

[8] L. Du, J. Huang, and Q. Liu, 'A Realization of Measurement Unit for Phasor Measurement Unit Based on DSP', in *2012 Asia-Pacific Power and Energy Engineering Conference*, Mar. 2012, pp. 1–3. doi: 10.1109/APPEEC.2012.6307689

[9] L. Du, J. Huang, and Q. Liu, 'A Realization of Measurement Unit for Phasor Measurement Unit Based on DSP', in 2012 Asia-Pacific Power and Energy Engineering Conference, Mar. 2012, pp. 1–3. doi: 10.1109/APPEEC.2012.6307689

[10] M. Sedlacek and M. Krumpholc, 'Digital measurement of phase difference - a comparative study of DSP algorithms', undefined, 2005, Accessed: Oct. 04, 2021. [Online]. Available: https://www.semanticscholar.org/paper/Digital-measurement-of-phase-difference-a-study-of-Sedlacek-Krumpholc/5a52d34e26eb2baf6bb2b9cf28e64034b66299a0

[11] S. Mondal, Ch. Murthy, D. S. Roy, and D. K. Mohanta, 'Simulation of Phasor Measurement Unit (PMU) using labview', in 2014 14th International Conference on Environment and Electrical Engineering, May 2014, pp. 164–168. doi: 10.1109/EEEIC.2014.6835857

[12] Modi, P. K. and S. Kamboj. "Modeling of phasor measurement unit (PMU) using various phasor estimation techniques in matlab." (2015).

[13] C. J. Pillay, M. Kabeya, and I. E. Davidson, 'Transmission Systems: HVAC vs HVDC', p. 17, 2020

[14] TekTalksengineered, HVDC Vs HVAC. Transmission System Comparison., (Aug. 31, 2019). Accessed: Sep. 18, 2021. [Online Video]. Available: https://www.youtube.com/watch?v=qbi0rufpCdI

[15] Francisco Gonzalez-Longatt, 1. Introduction to HVDC Systems. 'Seminar on DC transmission systems', (Apr. 15, 2020). Accessed: Oct. 06, 2021. [Online Video]. Available: https://www.youtube.com/watch?v=k69WlxwmgyI

[16] J. Setreus and L. Bertling, 'Introduction to HVDC Technology for Reliable Electrical Power Systems', in Proceedings of the 10th International Conference on Probablistic Methods Applied to Power Systems, May 2008, pp. 1–8

[17] R. Leelaruji, J. Setreus, G. Olguin, and L. Bertling, 'Availability Assessment of the HVDC Converter Transformer System', in Proceedings of the 10th International Conference on Probablistic Methods Applied to Power Systems, May 2008, pp. 1–8

[18] Y. Li, L. Luo, C. Rehtanz, K. Nakamura, J. Xu, and F. Liu, 'Study on Characteristic Parameters of a New Converter Transformer for HVDC Systems', IEEE Trans. Power Deliv., vol. 24, no. 4, pp. 2125–2131, Oct. 2009, doi: 10.1109/TPWRD.2009.2021033

[19] M. Daryabak et al., 'Modeling of LCC-HVDC Systems Using Dynamic Phasors', IEEE Trans. Power Deliv., vol. 29, no. 4, pp. 1989–1998, Aug. 2014, doi: 10.1109/TPWRD.2014.2308431

[20] 'Thyristor or Silicon Controlled Rectifier Tutorial', Basic Electronics Tutorials, Aug. 26, 2013. https://www.electronics-tutorials.ws/power/thyristor.html (accessed Sep. 22, 2021)

[21] M. Daryabak et al., 'Modeling of LCC-HVDC Systems Using Dynamic Phasors', IEEE Trans. Power Deliv., vol. 29, no. 4, pp. 1989–1998, Aug. 2014, doi: 10.1109/TPWRD.2014.2308431

[22] M. P. Bahrman and B. K. Johnson, 'The ABCs of HVDC transmission technologies', IEEE Power Energy Mag., vol. 5, no. 2, pp. 32–44, Mar. 2007, doi: 10.1109/MPAE.2007.329194

[23] B. Jacobson et al., 'HVDC with voltage source converters and extruded cables for up to±300 kV and 1000 MW', Nov. 2021

[24] 'Pulse Width Modulation (PWM) - Generation, Applications and Advantages', electricalfundablog.com, Jun. 23, 2019. https://electricalfundablog.com/pulse-width-modulation/ (accessed Oct. 07, 2021)

[25] P. Kundur, J. Paserba, V. Ajjarapu, G. Andersson, A. Bose, C. Canizares, N. Hatziargyriou, D. Hill, A. Stankovic, C. Taylor, T. Van Cutsem, and V. Vittal. Definition and classification of power system stability IEEE/CIGRE joint task force on stability terms and definitions. IEEE Transactions on Power Systems, 19(3):1387–1401, Aug 2004

[26] Joint Task Force on Stability Terms and Definitions, "Definition and Classification of Power System Stability", IEEE Transactions on Power Systems, Vol. 19, No.2, May 2004

[27] S. Y. S. Rajapakse and U. D. Annakkage, "Demonstration of voltage stability by comparing dynamic simulations and quasi steady state analysis," 2017 IEEE Electrical Power and Energy Conference (EPEC), 2017, pp. 1-4, doi: 10.1109/EPEC.2017.8286145

[28] J. Liu, M. Han and X. Chen, "Development of VSC HVDC quasi-steady-state model and its application," 2009 International Conference on Sustainable Power Generation and Supply, 2009, pp. 1-4, doi: 10.1109/SUPERGEN.2009.5347957

[29] L. He and C. Liu, "Parameter Identification With PMUs for Instability Detection in Power Systems With HVDC Integrated Offshore Wind Energy," in IEEE Transactions on Power Systems, vol. 29, no. 2, pp. 775-784, March 2014, doi: 10.1109/TPWRS.2013.2283656

[30] M. Grenier, D. Lefebvre and T. Van Cutsem, "Quasi steady-state models for long-term voltage and frequency dynamics simulation," 2005 IEEE Russia Power Tech, 2005, pp. 1-8, doi: 10.1109/PTC.2005.4524400

[31] Hans Kristian Hansen. Online Voltage Stability Monitoring in Distribution Networks, MSc Thesis, NTNU, 2017

[32] Dinh Thuc Duong. Online Voltage Stability Monitoring and Coordinated Secondary Voltage Control. PhD thesis, NTNU, 2016

[33] M. Begovic, B. Milosevic, and D. Novosel. A novel method for voltage instability protection. In Proceedings of the 35th Annual Hawaii International Conference on System Sciences, pages 802–811, Jan 2002

[34] Y. Wang, I. R. Pordanjani, W. Li, W. Xu, T. Chen, E. Vaahedi, and J. Gurney. Voltage stability monitoring based on the concept of coupled single-port circuit. IEEE Transactions onPower Systems, 26(4):2154–2163, Nov 2011

[35] Y. Lei, A. Mullane, G. Lightbody, and R. Yacamini, “Modeling of the wind turbine with a doubly fed induction generator for grid integration studies,” IEEE Trans. Energy Convers., vol. 21, no. 1, pp. 257–264, Mar. 2006

[36] Example Documentation, "HVDC Connected Offshore Wind Farm", DIgSILENT PowerFactory, 2021

[37] Example Documentation, "Nine-bus System", DIgSILENT PowerFactory, 2021

# Appendices

Table 3: Parameters of the 3-winding transformer

| Parameters | Values |
|---|---|
| HV-Side Rated Power | 240 MVA |
| MV-Side Rated Power | 120 MVA |
| LV-Side Rated Power | 120 MVA |
| Vector Group | YN0d5d5 |
| HV-Side Rated Voltage | 155 kV |
| MV-Side Rated Voltage | 33 kV |
| LV-Side Rated Voltage | 33 kV |

Table 4: Parameter of the VSC-Converter

| Parameter | Values |
|---|---|
| Type | Half-bridge type MMC |
| Rated AC Voltage | 155kV |
| Rated DC Voltage | 300kV |
| Rated Power | 450 MVA |
| Short Circuit Impedance | 10% |
| Copper Losses | 400 kW |
| No-load losses | 30000 kW |
| Resistance, $R_{arm}$ | 0.006 |
| Inductance $L_{arm}$ | 60mH |

Table 5: Parameter of the HVDC Line

| Parameter | Values |
|---|---|
| Rated Voltage | 150 kV |
| Rated Current | 5 kA |
| Length | 100 km |
| Resistance | 0.01 Ohm/km |
| Inductance | 1.27324 mH/km |

Table 6: Parameter of three phase transformer

| Parameters | Values |
|---|---|
| Type | YNd5 |
| Rated Power | 300 MVA |
| HV side voltage | 230 kV |
| LV side Voltage | 110 kV |
| Reactance x1 | 0.1099986 p.u. |
| Resistance r1 | 0.00055556 p.u. |
| Frequency | 50 Hz |

Table 7: Parameters of 5-MW DFIG

| Parameters | Values |
|---|---|
| Stator Resistance | 0.01 p.u. |
| Stator Reactance | 0.1 p.u. |
| Magnetizing Reactance | 3.5 p.u. |

| | |
|---|---|
| Rotor Resistance | 0.01 p.u. |
| Rotor Reactance | 0.1 p.u. |
| Acceleration Time Constant | 0.3762633 s |

Table 8: Parameters of Three Phase Transformer

| **Parameters** | **Values** |
|---|---|
| Connection | 3-ph Dyn5 |
| Primary Rated Voltage | 0.69 kV |
| Secondary Rated Voltage | 33 kV |
| Positive Sequence Reactance | 0.05999167 p.u. |
| Positive Sequence Resistance | 0.00099986 p.u. |
| Grounding Impedance | 0.1 ohm |
| Rated Power | 5.6 MVA |

Table 9: Parameters of NEC

| **Parameters** | **Values** |
|---|---|
| Rated Voltage | 33 kV |
| Rated Current | 0.1 kA |
| Zero Sequence Reactance | 0 Ohm |
| Zero Sequence Resistance | 750 Ohm |

Table 10: Nominal Bus Voltages

| Bus | Voltage (kV) |
|---|---|
| 1 | 16.5 |
| 2 | 18 |
| 3 | 13.8 |
| 4 | 230 |
| 5 | 230 |
| 6 | 230 |
| 7 | 230 |
| 8 | 230 |
| 9 | 230 |

Table 11: Generator Data

| Parameters | G1 | G2 | G3 |
|---|---|---|---|
| Nominal Apparent Power [MVA] | 247.5 | 192.0 | 128.0 |
| Nominal Voltage [kV] | 16.5 | 18.0 | 13.8 |
| Nominal Power Factor | 1.00 | 0.85 | 0.85 |
| Plant Category | Hydro | Coil | Coil |
| Rotor Type | Salient Pole | Round Rotor | Round Rotor |
| $x_d$[p.u.] | 0.3614 | 1.7199 | 1.6800 |
| $x'_d$[p.u.] | 0.1505 | 0.2300 | 0.2321 |
| $x_q$[p.u.] | 0.2328 | 1.6598 | 1.6100 |

| | | | |
|---|---|---|---|
| $x'_q$[p.u.] | 0.000 | 0.3780 | 0.3200 |
| $x_1$(leakage)[p.u.] | 0.0832 | 0.1000 | 0.0950 |
| $\tau'_{d0}$[p.u.] | 8.960 | 6.000 | 5.890 |
| $\tau_{q0}$[p.u.] | 0.000 | 0.535 | 0.600 |
| Inertia Constant H [s] | 9.5515 | 3.9216 | 2.7665 |

Table 12: Load Data

| **Load** | **P [MW]** | **Q [Mvar]** |
|---|---|---|
| Load A | 125 | 50 |
| Load B | 90 | 30 |
| Load C | 100 | 35 |

Table 13: Line Data

| **Line** | **R[Ω]** | **X[Ω]** | **B[μS]** |
|---|---|---|---|
| 4-5 | 5.2900 | 44.9650 | 332.70 |
| 4-6 | 8.9930 | 48.6680 | 298.69 |
| 5-7 | 16.928 | 85.1690 | 578.45 |
| 6-9 | 20.631 | 89.9300 | 676.75 |
| 7-8 | 4.4965 | 38.0880 | 281.66 |
| 8-9 | 6.2951 | 53.3232 | 395.08 |

Table 14: Transformer Data

| **Transformer** | **From** | **To** | **HV [kV]** | **LV [kV]** | **X1 [p.u.]** | **Rated Power [MVA]** |
|---|---|---|---|---|---|---|
| T1 | Bus 1 | Bus 4 | 230 | 16.5 | 0.1440 | 250 |
| T2 | Bus 2 | Bus 7 | 230 | 18.0 | 0.1250 | 200 |
| T3 | Bus 3 | Bus 9 | 230 | 13.8 | 0.0879 | 150 |